# An Analysis of Cricket Ball Swing using Computational Methods

Philip Eccleston

April 20, 2017

**Abstract**

In this project we attempt to explain the governing phenomena behind swing bowling and proceed to use OpenFOAM to obtain computational solutions for air flow problems around cricket balls. We analyse these results in relation to the theory behind swing bowling and compare how both the seam angle and release velocity affect the lateral force generated. We finally go on to use these results to create a spreadsheet model that predicts swinging trajectories.

## Contents

# 1 Introduction

At its heart, Cricket is a bat and ball game, yet it occupies an unusual place in the world of modern sports. Its endless customs and esoteric quirks coupled with the bemusing amount of time that matches can last make for endless intricacies and strategies which make the game both interesting to watch and study.

Beyond the conflict of two competing teams, at any individual instant in time cricket is a tense contest between 2 individuals; the batter and the bowler. The bowler propels the ball towards the batsman, and they endeavour to swat the ball away to score runs (points) by hitting the ball over the boundary line or by running between the sets of stumps. The batsman, however, is under the constant threat that he may be declared out by several different means; The most common ones being,

1. Bowled - The bowler is able to hit the stumps and dislodge the bails atop of them
2. Caught - The batsman hits the ball into the air and into the fielder's hands
3. Run out - The batsman and his partner attempt to run and the fielders are able to throw the ball at the stumps before they get to the opposite end.
4. LBW (Leg before Wicket) - The bowler bowls the ball and it hits the batsman's body when it would have gone on to hit the stumps

Once the batsman is out then they are no longer able to score runs for their team. The team's innings end once 10 of their batsman are declared out. In practice, however, getting a batsman out is not a simple task, often in test matches, a batsman may continue batting for hours with apparent ease. Alternatively, a batter may make the long walk out into the middle only to return to the changing rooms after a single delivery.

Throughout history, bowlers have tried a plethora of methods and tactics to get batsmen out and limit their run scoring opportunities. There are strategies so prominent that they are ingrained in cricket's folklore including Douglas Jardine's aggressive targeting of the batsman's body in the 1932-33 'Bodyline' series; the West Indies' unrelenting pace barrage of Roberts, Holding, Croft and Garner in the 1980s and Pakistan's reverse swinging duo of Wasim Akram and Waqar Younis in the 1990s.

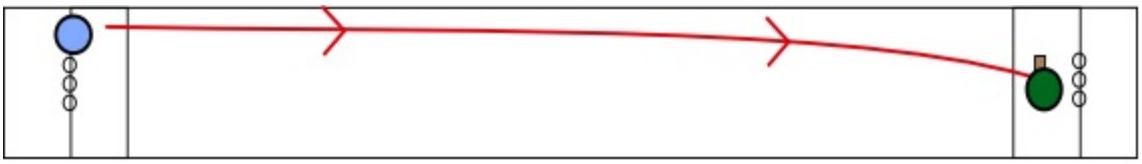

Figure 1: An example trajectory as viewed from above of a ball bowled by the player in blue which swings inwards towards the player in green

One of the crucial methods in a fast bowlers arsenal that is the focus of this project is the craft of swing bowling, a seemingly unintuitive curving of the ball through the air. We will be looking into the key mechanisms of this style of bowling and how it affects the ball in flight by finding computational solutions to the governing Navier-Stokes equations and analysing the resulting airflow. Then we will examine the controllable factors that a bowler may look to exploit and how best to maximise the magnitude of swing displacement and ultimately how to better the ability to claim a batsman's wicket.

## 1.1 Role of the ball within the game

Cricket is a complicated game with many rules and differing phases of play. Here we shall be concentrating upon what happens between the moments when the ball is 'bowled' by the bowler and the moment just before it reaches the batsman.

Although the overarching mechanism of bowling is the same, bowlers tend to fall into two main categories; spin bowlers and fast bowlers. Spin bowlers bowl the ball at speeds of between 20 and $26ms^{-1}$ $(45 - 58mph)$ primarily rely on imparting spin on the ball as to have it 'drift' through the air due to Magnus effect and then bounce and turn unexpectedly off the pitch as to lure the batsman into making a mistake. Fast bowlers bowl at speeds that vary from a low of around $32ms^{-1}$ (where they are fittingly referred to as medium pace) up to $42ms^{-1}$ $(72 - 94mph)$. Fast bowlers rely on their pace, and the ability to cause the ball to bounce unexpectedly off the seam and to 'swing' through the air to outfox a batsman.

This phenomenon of swing occurs due to complex asymmetric fluid behaviour causing a net horizontal force to be imparted on the ball, thus causing a deviation from its expected trajectory and resultantly attempts to deceive the batsman and causing them to mishit the ball or miss the ball entirely. This is commonly categorised as either outswing or inswing dependent on which direction the ball moves relative to the batsman. Inswinging deliveries generally start on a trajectory that would be far away from the batsman and then swings in towards them with the intent of hitting the stumps or trapping them on the crease L.B.W. Outswing acts in the other direction and intends to have the ball catch the edge of the bat and then provide a simple catch to a fielder.

Swing bowling is a fine art, and even the most experienced of players struggle to get consistent swing on the ball and in certain scenarios any lateral movement at all. There is a conventional wisdom among the cricket community that suggests how to generate swing, bowlers seeking this phenomenon concentrate on the position of the seam of the ball relative to the airflow; the roughness of one side of the ball compared to the other, which they will often affect by attempting to polish one side of the ball throughout the match and the atmospheric and pitch conditions.

There are two very similar phenomena that must also be mentioned at this stage, reverse swing and the recently coined contrast swing.

Reverse swing was brought to the forefront of the cricketing world in the early 1990s by the Pakistani fast bowling duo and Wasim Akram and Waqar Younis. This behaviour is identified as when the ball is angled in the same way to a conventionally swung delivery but instead moves in the opposite direction. This is a complex process and is hard to reproduce but it is usually seen once the ball has been in play for at least 20 overs and as a result has picked up markings and imperfections; had its seam flattened and the fielding team have had the chance to polish one side of the ball. Even with these ball conditions, this effect is generally only significant in bowlers who release the ball at speeds in excess of $40ms^{-1}$ (90mph). Many descriptions have been offered by fluid engineers and enthusiasts over the real mechanisms behind reverse swing such as those by Barrett and D.H Wood (1996), A. T. Sayers (2001) and Scobie et al. (2013). Each offering varying descriptions and opens up the possibility that multiple factors must culminate in order to produce substantial reverse swing in real world situations. It is currently understood that as the ball ages we encounter turbulent layers forming on both sides of the ball. These layers form at roughly the same point as each other, near the front of the ball. However in this instance, as the airflow passes over the seam the turbulent layer is predicted to both thicken and weaken. This makes it more susceptible to separate from the surface before the layer on the non-seam side separates. Thus creating an angled wake and a pressure difference across the ball which causes the swing force to act in the unexpected direction.

Contrast swing was first described by R. Mehta (2006a) and in a similar vain to reverse swing, is an effect that causes the ball to move in a way not concurrent with a conventional swing description. The inception of the term was due to bowlers swinging a new ball in the unexpected direction despite the ball not being conditioned in a way indicative of reverse swing. Example have also been highlighted where there is swing despite the seam being straight up and thus forming no angle with the airflow. This has currently been put down to minor imperfections in the ball or blemishes that have been picked up within the first few overs of play. There is limited academic research on this topic and currently there is no widely agreed theory backing this phenomenon.

### 1.2 Description of the Cricket Ball

Unlike many other Sports balls, Cricket balls are held to strict design specification described in a British standard *Specification for cricket balls* (1995). In terms of general construction, the ball is made up of 2 halves, with each half consisting of 2 quarters of leather internally stitched and the two halves joined together by a primary seam made up of 3 double rows of stitching with between 78 and 86 stitches in each row. with the seam height being between 0.5 and 0.9mm.

The Marylebone Cricket Club control and manage the laws of the game and Law 5 dictates the precise size and weight requirements for the ball, in the senior Men's game they stipulate tolerances for the mass (155.9g,163g) and the circumference (22.4cm,22.9cm)[1], and for this purpose, we will be working with values of 160g and 3.7cm for the mass and radius respectively in any future calculations.

## 2 Governing Phenomena

To begin to understand the motion of a cricket ball there are several key phenomena which must be at least qualitatively understood. These give a context from which to appreciate and understand the nature of swing bowling. The key feature we try to understand is the behaviour of the air flow and subsequent boundary

[1] *The Laws of the cricket: Law 5 the Ball* n.d.

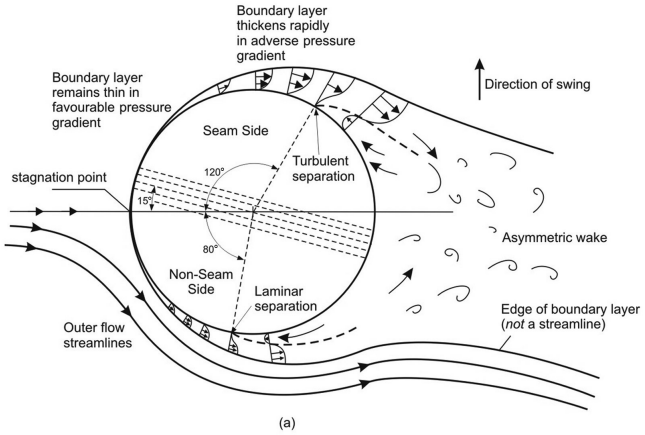


Figure 2: A diagram explaining boundary layer separation. (greatly exaggerated in thickness for clarity) Source: Scobie et al. (2013)

layers that form around either side of the ball. Then we must relate how this is influenced by seam position and release velocity and how this imparts a force on the ball, but other less obvious phenomena such as the Magnus effect and the effect of drag must also be considered to fully explain the trajectory of the ball while in the air.

## 2.1 Boundary Layers

There is general consensus about the main mechanism for the swing phenomena as first laid out by Cooke (1955). With many of the early practical experiments performed by R. D. Mehta (1985) and Barton (1982) providing evidence to this hypothesis. It is currently understood that the effect of angling the raised seam so that it points at a shallow angle to the incoming airflow causes the air to behave differently on either side of the ball. On both sides, we get the air separating into 2 distinct areas, a laminar flow and a more turbulent region found between this flow and the surface of the ball.

However, the point at which the turbulent layer separates varies on either side. On the half of the ball which the seam points into, as the air flow passes over the raised surface of the stitches the flow immediately next to the ball's surface is tripped from a laminar flow to a thin layer of turbulent flow. Whereas on the non-seam side, initially the air is travelling around the relatively smooth side of the ball and thus the flow remains laminar until the point where it separates from the ball. By merit of it's increased energy the turbulent layer stays attached to the surface of the ball for longer before separating away from the surface. This has the result that a low-pressure asymmetric wake is induced behind the ball and due to this a pressure differential and thus a net force exists perpendicular to the flow. It is this force which causes the ball to move with an unexpected curve in one direction or the other in the phenomena known as swing.

The formation of this turbulence layer can be affected further if the surface of the ball is rougher on one side than the other as this acts much in the same way as the seam and causes the turbulent layer to form more readily resulting in a lower pressure on that side of the ball and thus exhibit greater displacement.

## 2.2 Drag Forces

As the ball moves through the air its velocity decreases due to the effect of drag. This force arises due to the pressure difference between the high pressure caused by the flow colliding with the front of the ball and the low pressure found in the turbulent wake which forms behind the ball. Our computational model will allow us to find explicit values for this pressure difference and thus the net force that pulls the ball backwards.

We can give a rough insight into the magnitude of this force by modelling the ball as a perfect sphere, and then using the drag equation with known values.

$$F_d = \frac{1}{2}\rho u^2 C_d A$$

Where $C_d$ is the drag coefficient which varies dependent upon Reynolds number, and A is the appropriate reference area which for a sphere is $\pi r^2$. We make the prediction here that a typical Reynolds number in our set up is between $4 \times 10^4 < Re < 2 \times 10^5$ as used in experiments by A. Sayers and Hill (1999) for which measured forces gave $C_d \approx 0.5$. Which is in agreement with the drag coefficient of a sphere in similar air flows Franzini, Finnemore, and Daugherty (1997). Thus inputting our values for a cricket ball of radius 3.58cm travelling at $39ms^{-1}$ we get that the drag force is $F_d = 1.88N$, giving an acceleration on the ball of $-12.6ms^{-2}$.

Simplified calculations that assume this is a constant force then give us that as the ball travels the 18.3m (20 yards) down the wicket, this force will cause the ball to slow down to a velocity of $33ms^{-1}$ (73mph) by the time it reaches the batsman. This calculation doesn't account for the decrease in the drag force as the ball decelerates. Thus the real life observed speed we expect to be greater than this. Regardless, this does highlight that the ball's velocity changes greatly enough from the point of release to point of impact that it may have an impact on swing and is worth reconsidering this when we analyse the relation between swing displacement and bowling speed later on.

## 2.3 Magnus Effect

The Magnus effect is a phenomenon that can be observed readily in sports. When an object such as a ball or cylinder is spinning through a fluid then there is a force generated which causes the object to curve through the air. This is the principle behind curving free kicks in football, backspin to maximise drive distance in golf and drift when spin bowling in cricket.

It is important to mention that drift caused by the Magnus effect is distinct from the effects that lead to swing. Instead, the Magnus effect does play a subtle role in fast bowling. Due to the biomechanics of a fast bowling action, there is a natural tendency to impart backspin on the ball when released. This backspin generates a lift force that acts against gravity and thus causes the ball to remain in the air for longer and thus will land closer to the batsman than they may be expecting.

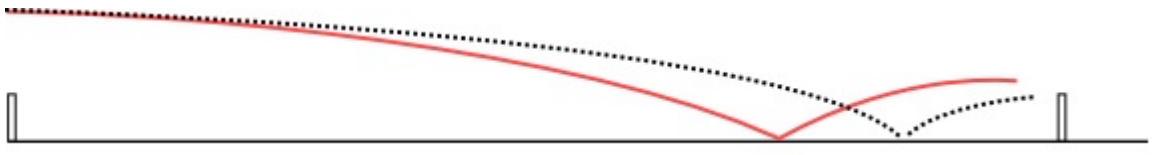

Figure 3: A side on view of a ball bowled without backspin (red) and one bowled with back spin (dotted)

A. Sayers and Hill (1999) obtained measured values for the lift on a ball mounted on a sting and placed in a wind tunnel at varying rotational speeds. They obtained a lift force of between 0.3N and 0.5N for balls with spin rates in the range 63 to 104 rad/s placed in air flows between 30 and $35ms^{-1}$. The tested angular velocities are concurrent with values generated by bowlers as backed up by research by Cork, Justham, and West (2013), who investigated measuring spin rates produced by 10 different fast-medium bowlers using high speed cameras, and calculated a mean spin rate of 82 rad/s with a large standard deviation of $\pm 35$ rad/s.

Under the assumption that spin deterioration in negligible over the course of the ball's flight we can obtain rough values for the effect of backspin on the flight of the ball. For a ball released horizontally at 2m above the ground at $32ms^{-1}$ without backspin we would expect to travel 20.4m down the wicket before hitting the ground, whereas a ball with backspin we would expect to travel 23.7m. A significant enough difference that despite the avoided complications serves to show that the back spin on the ball and the subsequent force due to Magnus effect has an influence to the order of meters as to where the ball lands on the pitch. Thus we must also consider this force when we will attempt to predict trajectories later on.

A more theoretical approach was taken by G. Robinson and I. Robinson (2015). They predicted the Magnus force by investigating the value of the lift coefficient as a function of the Reynolds number of the flow.

$$F_L = \frac{1}{2}\rho A C_L V \cdot (\frac{\boldsymbol{\omega} \times \boldsymbol{V}}{\omega})$$

Where $\rho$ is the air density, $\boldsymbol{\omega}$ is the angular velocity vector of magnitude $\omega$, A is the cross-sectional area of the ball and V is the airspeed. $C_L$, the lift coefficient, is a scaling value unique to the ball and based on results from their earlier 2013 work on golf balls and baseballs they assumed $C_L$ to vary as.

$$C_L = 0.54(\frac{\omega r}{V})^{0.4}$$

Which they obtained from Smits and Smith's 1994 work on lift coefficients for golf balls, arguing that it used a similar range for V and $\omega$ as we see in Cricket games and it was both comparable and more reliable than other proposed formulae. We can then work from this to develop a theoretical lift force on a rotating ball. In order to compare directly with Sayers' experimental lift value, we shall calculate the lift force for a ball travelling at $30ms^{-1}$ rotating at 800rpm (83.8 rad/s) about its seam. Substitution of these values give $F_L = 0.484N$ which is comparable to the measured value of 0.4N obtained by Sayers. Robinson and Robinson also noted that as the rotational of the ball normally lines up with the seam that if we begin to angle the seam to the air flow there will be lift component acting in the perpendicular direction during the balls flight. This force would apply in addition to any swing force although their calculations reveal that for a spin rate of $100rads^{-1}$ for ball travelling at $38.8ms^{-1}$ (140kph) that this additional force increases with the seam angle but only corresponds to a displacement of 2.5cm at the point of impact for their maximum angle of 30° . A small but not necessarily negligible displacement, and potentially the difference between hitting the middle or the edge of the bat.

This pair also commented that fast bowlers who have a 'slingy' bowling action, that is releasing the ball with the arm at an angle to the vertical, may still be able to impart spin down the seam of the ball, but as the seam is now off-kilter we will now have a horizontal component to our lift force that may serve to amplify the effects of the swing force.

## 2.4 Atmospheric Conditions

There is a widely held belief that the ability to generate swing is affected by the weather, specifically that it is easier to generate when there is greater cloud cover. There has been considerable inconclusive discussion

about whether this perception is in fact valid and explanations offered as to why cloud cover may affect swing.

In our calculations the only relevant quantities that may be altered by cloudy more humid conditions are the dynamic viscosity of the air and the density of the air. These values affect the Reynolds number, Re.

$$Re = \frac{inertial forces}{viscous forces} = \frac{\rho U L}{\mu}$$

Where $\rho$ is the density of the air, U is the velocity of the ball, L is the characteristic linear dimension (taken to be the diameter of the ball here) and $\mu$ is the dynamic viscosity of the air.

The Reynolds number is a dimensionless quantity that compares the relative importance of forces in the fluid. It is most commonly used to define the characteristic nature of a flow; high Reynold number flows exhibit turbulent characteristics and lower numbered flows being laminar in nature. The flow behaviour has a direct impact on how our flow separation forms and on quantities like the drag coefficient.

We can derive the Reynold number equation from the momentum equation for a compressible flow.

$$\rho \frac{Du}{Dt} = -\frac{\delta p}{\delta x} + \nabla \cdot (\mu \nabla u) + F_x$$

$$\frac{\delta \rho u_i}{\delta t} + \frac{\delta}{\delta x_j}(\rho u_i u_j + p\delta_{ij}) = \mu \frac{\delta^2 u_{ij}}{\delta x_i \delta x_j}$$

At this point, we non-dimensionalise the variables by dividing through by some reference values. U, L and $\rho$ giving new variables, $\bar{x} = \frac{x}{L}, \bar{u} = \frac{u}{U}, \tau = t\frac{U}{L}$ and $\bar{p} = \frac{p}{\rho u^2}$. Substituting these gives;

$$\frac{\delta U \bar{u}}{\delta \tau \frac{L}{U}} + U\bar{u}\frac{\delta U \bar{u}}{\delta L \bar{x}} = -\frac{1}{\rho}\frac{\delta \bar{p} \rho U^2}{\delta L \bar{x}} + \mu \frac{\delta^2 \bar{u}}{\delta \bar{x}^2}$$

We can now rearrange, grouping together terms that represent the effect of inertial forces and divide through by $\frac{U^2}{L}$ to give.

$$\frac{\delta \bar{u}}{\delta \tau} + \bar{u}\frac{\delta \bar{u}}{\delta \bar{x}} + \frac{\delta \bar{p}}{\delta \bar{x}} = \frac{\mu}{\rho U L}\frac{\delta^2 \bar{u}}{\delta \bar{x}^2}$$

Then we see that the term on the right-hand side corresponds to $\frac{1}{Re}$ and hence taking the ratio of inertial forces to viscous forces gives the Reynolds number equation.

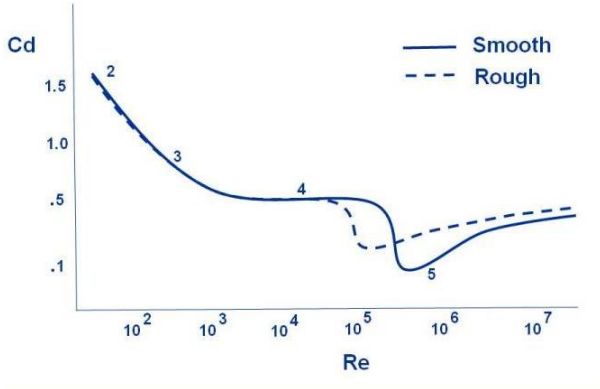


(a) The measured drag coefficient for a perfect sphere for varying Reynold numbers. Note the point of divergence between rough and smooth spheres is similar to typical Reynold's numbers found in Cricket ball flows.

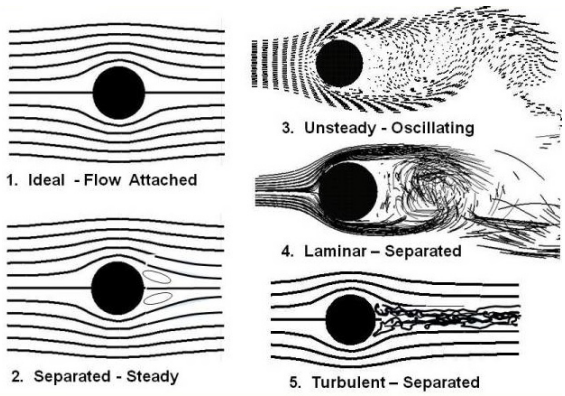


(b) Characteristic flows around cylinders for varying Reynold numbers. Our flows will mostly fall under the 4th category.

We can attempt to estimate the nature of our flow by taking typical values for these variables, $\rho$=1.225 kg $ms^{-1}$, U = 38 $ms^{-1}$, L = 7.2cm and $\mu = 1.983 * 10^{-5}$ Pa which gives a value of $Re \approx 1.7 \times 10^5$. Changes in the humidity and density of the air will alter this value somewhat, but calculations factoring in realistic changes of these values lead to a change of less than 2% (K. Bentley and Mehta. 1982). Thus we should not predict that our model will be able to account for this.

There are many other reasons proposed by Binnie (1976), K Sherwin (1982), James, MacDonald, and Hart (2012) as to why atmospheric conditions might affect swing, proposing respectively; 'Condensation shock' that would occur at the point of minimum pressure although calculations yielded that this would require a relative humidity of nearly 100%; humid days may have less inherent turbulence in the air and that it is the cloud cover, not humidity that is responsible for less turbulence due to smaller convection currents near the ground caused by the sun. However, all of these suggestions remain inconclusive after calculations predict a negligible impact on the ball.

# 3 Computations

Since the emergence of mathematics to describe the flow of fluids there have developed three main approaches to solve real-world problems: computationally, theoretically and experimentally and the role and importance of these methods have adapted with the advent of new technology. From derivation starting from Newton's laws, mass conservation and the laws of Thermodynamics it is possible to write the governing equations for a 3 dimensional incompressible fluid as;

$$\nabla \cdot \mathbf{u} = 0$$
$$\rho \frac{D\mathbf{u}}{Dt} = -\nabla \mathbf{p} + \mu \nabla^2 \mathbf{u} + \mathbf{F}$$

Where $\rho$ is density; $\mathbf{u}$ velocity; p pressure; $\mu$ dynamic viscosity and $\mathbf{F}$ the body forces.

These are the Navier-Stokes equations and it is generally not possible to solve these analytically except in some very simple cases. Thus to solve the complex problem of air flow around a cricket ball we are taking a computational approach and utilising the open source software 'OpenFOAM' to provide the framework to do so. We must firstly define the geometry of the problem by creating a model cricket ball and generating a mesh, a vast array of coordinates which serve to discretise the domain and then further specify the initial and boundary conditions of the set-up.

Secondly, we then use an algorithm to solve the governing equations of the fluid flow at all points in the mesh and at subsequent discrete time increments.

The justification for computational fluid dynamics is that by solving the flow problem on a large number of discrete points in both time and space that the solution is an accurate representation of the real world problem. The solution then may be analysed as if a true realisation of the problem.

## 3.1 Model of Cricket Ball

a CAD model of the ball was made using the FreeCAD software. Its dimensions based on the standard described earlier consisting of a sphere of radius 36mm. 6 lines consisting of 80 stitches each were then added

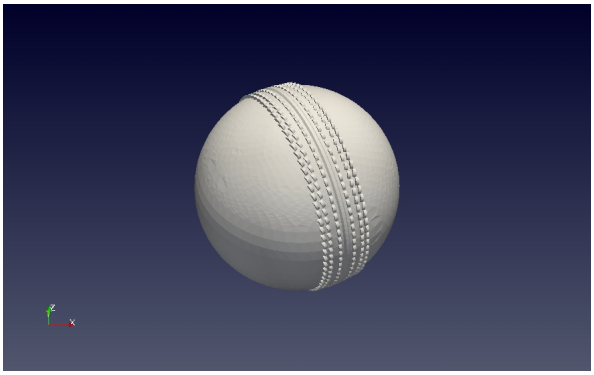

(a) The CAD model of the ball

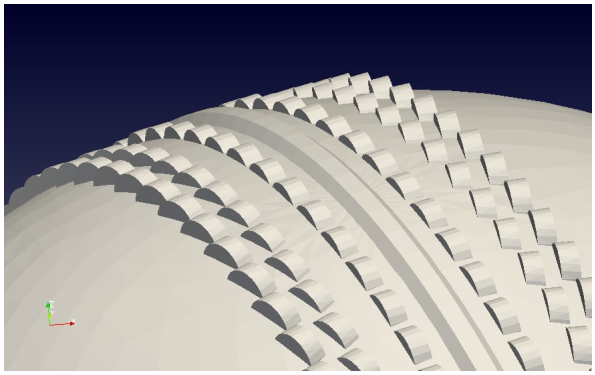

(b) Detailed close up of the seam

around the circumference of the ball to mimic the seam. The stitches consist of 1mm high cylinders set into the surface of the ball. A further cylinder of radius 36.5mm and height 3.6mm was added, whose edges were then both chamfered in order to simulate the raised leather between the two hemispheres that is found on most balls.

## 3.2 Meshing

There are several key features that needed be noted when developing the mesh for the simulation. Firstly, the mesh needed to be fine enough, that is, it must contain enough points that solving the equations on the mesh is comparable to the real life solution. However, a finer mesh requires much greater computing power and thus a compromise must be met. Thus, We chose to implement a finer mesh near areas of interest, these include; near the surface of the ball; around the seam of the ball and in the immediate wake of the ball. This is then balanced out by having a coarser mesh once we are away from these areas.

The OpenFoam command blockMesh was used to generate an initial cuboid with height and width 100mm and length 300m, and a simple 20x20x40 cube based mesh within. Then our CAD cricket ball was placed at the centre of the domain. We next implemented the command surfaceFeatureExtract, this generated an .eMesh file which specifies the edges of the cricket ball model and specifically highlights edges which may cause issues, these are normally where the model may have sharp angles between faces which may not be meshed accurately unless specifically accounted for.

snappyHexMesh was then used to refine the mesh around the surface of the ball. snappyHexMesh works by continual splitting of the cuboid cells generated by blockMesh which are near to the surface of the ball, thus making the mesh finer in our area of interest and changing the cell shape from cuboids to a variety of hexahedra and split-hexahedra. Next, it removes any parts of the cells that intersect the surface of the ball and snaps the remaining cells to the surface of the model. Then it refines the nearby cells according to a large range of inputted parameters in order that the cells don't become too small, distorted or act in any way which may adversely affect the accuracy of the model.

In order to model the air flow behind the ball, we also specified two separate refinement regions. The first one was in the form of a cuboid with dimensions $10 \times 20 \times 10$cm, where one of the $10 \times 10$cm faces is centred on the middle of the ball and the other face set 20cm further down the stream. In this region we specified an increased level of refinement thus increasing the resolution of the mesh in that area. The second region was a sphere or radius 5cm centred on the ball in which the mesh was refined one level finer than the box. These

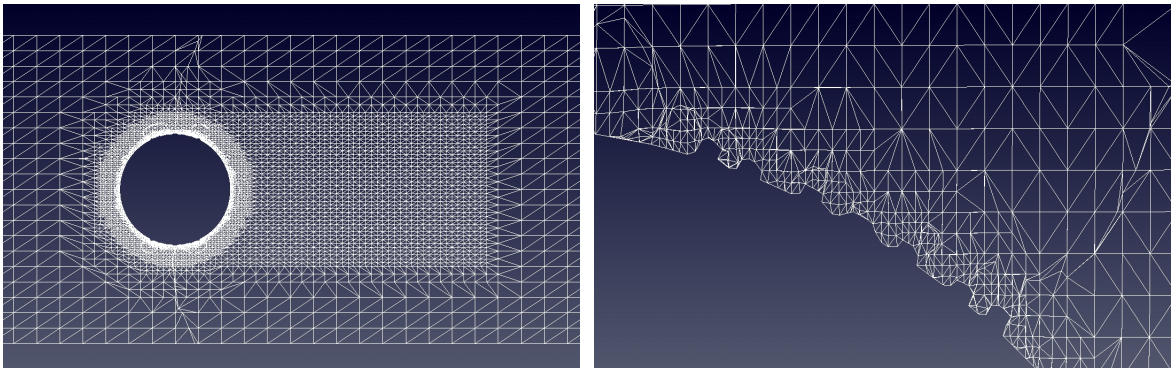

(a) A slice through the mesh in the XY plane

(b) Detailed close up of mesh around the seam

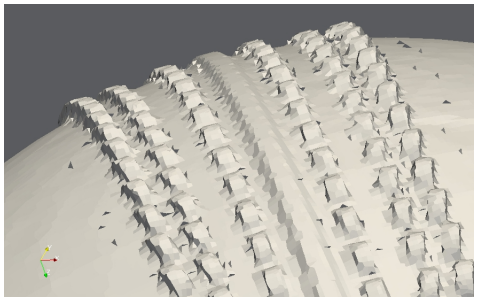

Figure 7: The mesh used still maintained the seam detail

regions not only allowed us to visualise the air behaviour around and behind the ball but also this allowed any of the resulting vortices and flow in the wake to affect the airflow around the surface in ways that are expected but would not be acknowledged by a coarser mesh.

### 3.3 Solver

All calculations were performed with the SimpleFoam solver that comes packaged with OpenFOAM, This is built off the SIMPLE algorithm developed by Patankar and Spalding (1972). At its core, it is a steady state solver that uses the finite volume method to calculate solutions to the Navier-Stokes equations under the restriction that the flow is incompressible.

The governing equations of fluid flow are derived from three conservation laws; In a small volume of fluid the mass of the fluid is conserved; The rate of change of momentum is equal to the sum of the acting forces (Newton's Second Law) and that the rate in the change of energy is equal to the rate of work done on a particle in addition to the sum of the rate of heat addition (1st Law of Thermodynamics). In our model, we will also make some assumption of the nature of fluid at hand, air. Firstly that, in our scenario air is incompressible and that it behaves like a Newtonian fluid. the Newtonian fluid descriptor relates to a property of the fluid called its viscous stress. This is what describes the notion of viscosity of a fluid, and from a simple perspective can be thought of the inherent internal friction, that when a fluid particle moves there is some resistance to this motion by neighbouring particles. This resistance is represented mathematically as a tensor $\tau_{ij}$ denoting the corresponding direction. A Newtonian fluid states that these viscous stresses are proportional to the rate at which the fluid deforms. This is stated mathematically as;

$$\tau_{ii} = 2\mu\frac{\delta \mathbf{U}_i}{\delta i} + \lambda\nabla\cdot\mathbf{U} \qquad \text{for i=x,y,z}$$

$$\tau_{ij} = \tau_{ji} = \mu(\frac{\delta U_i}{\delta j} + \frac{\delta U_j}{\delta i}) \quad \text{for i,j=x,y,z}$$

Here, $\mu$ is the dynamic viscosity and relates stresses to linear deformations and $\lambda$ relates stresses resulting from volumetric deformations. However, in our incompressible case, $\nabla\cdot\mathbf{U} = 0$ and thus we can ignore $\lambda$.

The incompressible stipulation also simplifies the energy conservation equation as well. It turns out that without variation in the density of a fluid that there is no link between the energy conservation and the equations governing mass and momentum, (unless we were considering heat transfer in our model). Thus we can concentrate on just the mass and momentum equations.

From these laws, we can derive the Navier-Stokes equations, which are stated here in a form most useful for computational methods. (Here $\mathbf{F}$ describe the acting body forces)

$$\begin{aligned}
\nabla\cdot\mathbf{u} &= 0 \\
\rho\frac{Du}{Dt} &= -\frac{\delta p}{\delta x} + \nabla\cdot(\mu\nabla u) + F_x \\
\rho\frac{Dv}{Dt} &= -\frac{\delta p}{\delta y} + \nabla\cdot(\mu\nabla v) + F_y \\
\rho\frac{Dw}{Dt} &= -\frac{\delta p}{\delta z} + \nabla\cdot(\mu\nabla w) + F_z
\end{aligned}$$

It still remains to justify that in our scenario that the fluid may be assumed to be incompressible. This notion ultimately stems from the maximum air speeds that we shall expect to encounter in our simulation are around $60ms^{-1}$ ($\approx$ 134mph) this gives a corresponding Mach number of $M = \frac{60}{340} \approx 0.17$ which is considerably less than Mach number of 0.3[2] generally considered to be the threshold for which the effects of compressibility have a more than negligible impact. A brief justification of this can be given by looking at how the Mach number affects changes in the fluid density. Starting from the conservation of momentum equation for a steady flow:

$$\begin{aligned}
\rho\frac{Du}{Dt} &= -\frac{\delta p}{\delta x} + \nabla\cdot(\mu\nabla u) + F_x \\
\rho u\frac{du}{dx} &= -\frac{dp}{dx} \\
\rho u du &= -dp
\end{aligned}$$

We must now bring in two relations firstly the equation for Isentropic flow and secondly the speed of sound in an ideal gas. ($\gamma$ is the specific heat ratio of the medium)

$$\frac{dp}{p} = \gamma\frac{d\rho}{\rho}$$

$$c_{ideal} = \sqrt{\frac{\gamma p}{\rho}}$$

$$\Rightarrow dp = -c^2 d\rho$$

And by combining these relations and by the definition of the Mach number $M = \frac{u}{c}$

[2]This corresponds to a pressure change of 10% from the above calculations.

$$\Rightarrow \rho u du = c^2 d\rho$$

$$\Rightarrow \rho M^2 = d\rho$$

Center (2017b)

As seen, substituting in the value for M=0.17 shows that for the largest change in velocity we see that the corresponding the pressure change is less than 3% . We claim that this is negligible and thus an incompressible model is sufficient.

There are three primary types of solvers utilised to solve the Navier-Stokes equations based on how they go about discretising and then solving from the Mesh. These are the finite difference method, the finite volume method and the finite element method. The SimpleFoam algorithm is based on the finite volume method (FVM).

FVM is similar in concept to the notion of control volumes encountered in analytic fluid dynamics. It looks at the variables of interest (which in our case are p and u along with k,$\tilde{V}$,$\omega$ which relate to our turbulence model) and performs numerical integration of the governing equations evaluated at the centroid of the cell for a specific time. We then need to work out what the values of our variable are at the intersection points of our mesh. To do this, an interpolation profile is used to approximate the value at the nodes of the mesh based on the values of nearby centroids.

SimpleFoam has several other properties that make it the solver of choice. being based on the FVM, it has the additional property that regardless of the mesh used, the results satisfy conservation of mass, momentum and energy. It is a segregated solver, meaning that for each time step it solves for each variable independently over the entire domain, as a result, it supports parallel computing which allows large decreases in computation times. It also has an integrated feature in that it solves 'under-relaxation' meaning that each variable is updated according to

$$V_i^{New,Used} = V_i^{Old} + \alpha(V_i^{New,Predicted} - V_i^{Old})$$

Where $V_i$ is any of the concerned variables and $\alpha$ is the under-relaxation factor. Where a value of $\alpha$=1 would mean we just use the predicted value each iteration whereas a lower value would mean that the variable is less likely to diverge (and is thus more stable) at the expense of the solution converging more slowly. In our model we set the relaxation factor as 0.9 for U, and at 0.7 for both k and $\omega$. Online (2005a)

For completeness we include the order of operations for the SIMPLE algorithm.

- Set the boundary conditions for the time step.
- Solve the discretised momentum equation to compute the intermediate guessed velocity field.
- Compute the mass fluxes at the cells faces.
- Solve the pressure correction equation and apply under-relaxation.
- Correct the mass fluxes at the cell faces.
- Correct the velocities on the basis of the new pressure field.
- Solves all other discretised transport equation, these include all the turbulence variables.

- Update the boundary conditions to the new solved values.
- Repeat with newly calculated boundary condition until convergence.

### 3.4 Turbulence model

We also couple SimpleFoam with the kOmegaSST turbulence model, the Shear Stress Transport K-$\omega$ turbulence model. The need for such a model stems from disparities between Navier-Stokes solutions and observed air flows. In real life, we observe seemingly randomly forming vortices. Due to the quasi-chaotic nature of this turbulence it isn't possible to accurately incorporate turbulence. Instead, CFD utilises models that predict how turbulence may influence our solution. In our simulations we will use the KOmegaSST model, a Linear eddy viscosity model which is based off the Reynolds-averaged Navier-Stokes equations. These are the standard Navier-Stokes equations with the flow variables replaced by the sum between their mean and anticipated fluctuations. I.e, $\mathbf{u} = \mathbf{U} + \mathbf{u\prime}$ and $p = P + p\prime$. Giving

$$\nabla \cdot \mathbf{U} = 0$$
$$\frac{\delta U}{\delta t} + \nabla \cdot (U\mathbf{U}) + \nabla \cdot \overline{(u\prime \mathbf{u}\prime)} = \frac{1}{\rho}\frac{\delta P}{\delta x} + \mu \nabla \cdot (\nabla U)$$
$$\frac{\delta V}{\delta t} + \nabla \cdot (V\mathbf{U}) + \nabla \cdot \overline{(v\prime \mathbf{u}\prime)} = \frac{1}{\rho}\frac{\delta P}{\delta y} + \mu \nabla \cdot (\nabla V)$$
$$\frac{\delta W}{\delta t} + \nabla \cdot (W\mathbf{U}) + \nabla \cdot \overline{(w\prime \mathbf{u}\prime)} = \frac{1}{\rho}\frac{\delta P}{\delta z} + \mu \nabla \cdot (\nabla W)$$

Here the over lines denote a particular method of taking the time average of a variable. We observe that this essentially introduces a new term into the set of equations. The third term in each equation represents the momentum transfer due to these turbulent fluctuations in the flow. We can expand these terms and represent them as the Reynolds stresses, turbulent stresses resulting from the perturbation, that they represent. For the x-momentum equation we get;

$$\frac{\delta U}{\delta t} + \nabla \cdot (U\mathbf{U}) = \frac{1}{\rho}\frac{\delta P}{\delta x} + \mu \nabla \cdot (\nabla U) + \frac{1}{\rho}[\frac{\delta(-\rho\overline{(u\prime^2)})}{\delta x} + \frac{\delta(-\rho\overline{(u\prime v\prime)})}{\delta y} + \frac{\delta(-\rho\overline{(u\prime w\prime)})}{\delta z}]$$

As the principle set of equations to be solved.

This model utilises two additional equations to model the turbulent properties of our flow. It requires two more variables the turbulent kinetic energy, k and the specific turbulent dissipation. rate, $\omega$. We then track how this energy fluctuates. This model's strength combines the k-$\omega$ model and the k-$\epsilon$ model in a way which plays to their respective strengths.

If we consider our flow around the ball we can split this into two basic regions, the shear flow outside the boundary layer and the flow inside the boundary layer. Within the boundary layer the model uses the k-$\omega$ model since the anecdotal comparisons to

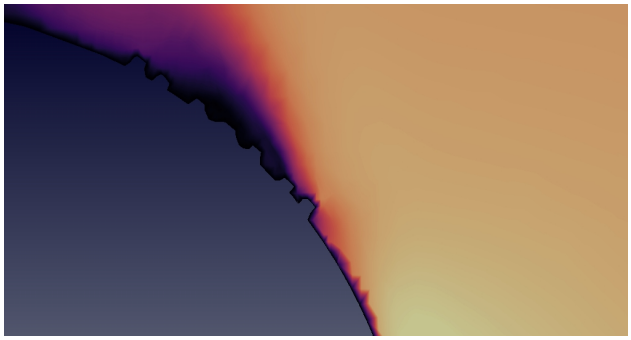

Figure 8: Close up of the flow separating and the formation of a boundary layer near the seam for the 40° ball at $34ms^{-1}$. Coloured according to the magnitude of the velocity

empirical data shows that it more accurately models
turbulence in areas of large pressure difference and more accurately predicts flow separations, but has the downside that it seems to be too sensitive to model the turbulence present in the free flow outside of the boundary layer; It is at this point the model switches to a k-$\epsilon$ model, which is thought to be more accurate in this circumstance.

The model tracks k as it is transported throughout the flow and is thus found according to

$$\frac{\partial k}{\partial t} + U_j \frac{\partial k}{\partial x_j} = P_k - \beta^* k\omega + \frac{\partial}{\partial x_j}[(\nu + \sigma_k \nu_t)\frac{\partial k}{\partial x_j}]$$

and $\omega$ via

$$\frac{\partial \omega}{\partial t} + U_j \frac{\partial \omega}{\partial x_j} = \alpha S^2 - \beta\omega^2 + \frac{\partial}{\partial x_j}\left[(\nu + \sigma_\omega \nu_T)\frac{\partial \omega}{\partial x_j}\right]$$

$$+2(1 - F_1)\sigma_{\omega 2}\frac{1}{\omega}\frac{\partial k}{\partial x_i}\frac{\partial \omega}{\partial x_i}$$

Where the coefficients are

- $CD_{k\omega} = \max\left(2\rho\sigma_{\omega 2}\frac{1}{\omega}\frac{\partial k}{\partial x_i}\frac{\partial \omega}{\partial x_i}, 10^{-10}\right)$
- $\phi = \phi_1 F_1 + \phi_2(1 - F_1)$
- $\alpha_1 = \frac{5}{9}$
- $\alpha_2 = 0.44$
- $\beta_1 = \frac{3}{40}$
- $\beta_2 = 0.0828$
- $\beta^* = \frac{9}{100}$
- $\sigma_{k1} = 0.85, \sigma_{k2} = 1$
- $\sigma_{\omega 1} = 0.5, \sigma_{\omega 2} = 0.856$
- $F_2 = \tanh\left[\left[\max\left(\frac{2\sqrt{k}}{\beta^*\omega y}, \frac{500\nu}{y^2\omega}\right)\right]^2\right]$
- $P_k = \min\left(\tau_{ij}\frac{\partial U_i}{\partial x_j}, 10\beta^* k\omega\right)$
- $F_1 = \tanh\left\{\left\{\min\left[\max\left(\frac{\sqrt{k}}{\beta^*\omega y}, \frac{500\nu}{y^2\omega}\right), \frac{4\sigma_{\omega 2}k}{CD_{k\omega}y^2}\right]\right\}^4\right\}$

F. R. Menter (1994) Online (2005b) F. R. Menter (2009). Note: OpenFOAM uses a slight modification based on the above based on the improvements proposed in F. Menter, Kuntz, and Langtry (2003).

For practical purposes, this requires us to specify a third new variable in our boundary conditions, the modified turbulent viscosity, $\tilde{\nu}$. This is calculated under the normal k-$\omega$ model as $\tilde{\nu} = \frac{k}{\omega}$. This definition is then complicated when we factor in scenarios where we use the k-$\epsilon$ model instead, in this case we define

$$\tilde{\nu} = \frac{a_1 k}{\max(a_1\omega, SF_2)}$$

where S is the modulus of the mean rate-of-strain tensor which features in the k-$\epsilon$ model calculations. The boundary conditions for this are not set for our domain bounding box but on the ball's surface we use the nutkWallFunction to specify that we use the calculated values of $\tilde{\nu}$ at these points.

In our initial conditions we must estimate a value for the turbulent kinetic energy and turbulence dissipation rate. These values hinge on the Reynolds number of our flow, We refer again to A. Sayers and Hill (1999) who predicted the typical values to be in the range $4 \times 10^4 < Re < 2 \times 10^5$ and R. Mehta and D Wood (1980) who estimated the critical value of the Reynolds number to be $1.5 \times 10^5$. We will work with this second value. For characteristic flows relating to such a Reynolds number we must now estimate the scale of any turbulent fluctuations in relation to the airflow.

We use an estimate of 3% for the Turbulence intensity which is defined as $I = \frac{u'}{U}$, Where u' is the RMS of the turbulent velocities and U is the mean velocity of the flow (taken to be $35ms^{-1}$). We can then work

these back to find both the turbulence kinetic energy, k and the Specific turbulence dissipation $\omega$. There are two further values we need to consider, the turbulence scale length which is taken to be the diameter of the ball (0.07m) and the kinematic Viscosity of the air which by referring to reference tables is found to be approximately $1.5 \times 10^5$. We can find k from the definition of u'.

$$UI = u' = \sqrt{\frac{1}{3}(u'^2_x + u'^2_y + u'^2_z)} = \sqrt{\frac{2}{3}k}$$

$$\frac{3}{2}(UI)^2 = k \Rightarrow k = 1.65$$

The specific turbulent dissipation represents the rate at which the turbulent kinetic energy is converted back into internal heat energy per unit volume and time. It is often estimated as

$$\omega = \frac{\sqrt{k}}{l} \rightarrow \omega = \frac{\sqrt{1.65}}{0.07} = 18.4$$

Giving us final values of k=1.65 and $\omega = 18.4$. It is important to note that these values will be calculated differently for different velocities of the flow due to the relative size of the turbulence fluctuations when compared to the incoming airflow. For simplicity however, we will take the values corresponding to $U = 35ms^{-1}$ in all circumstances.

## 3.5 Initial Conditions

Our initial velocity in our system is set to be uniform across the domain. This neglects any motion due to the ball slowing down through the air and doesn't factor in that the ball will be also be accelerating vertically. As most professional fast bowlers tend to average between 79-88mph (35-39$ms^{-1}$) the initial flow velocity was set to be $36ms^{-1}$ (81 mph).

The initial pressure is defined uniformly across the domain to be 0. We are able to do this since the incompressible Navier-Stokes equations are only dependent upon the pressure gradient and not the absolute value of the pressure, thus we can set our reference pressure to be zero. Hence explaining why we can see negative values for pressure in our results. We can recover our equivalent measured pressure values simply by changing our reference pressure to be 1atm and then adding on our pressure field once having multiplied through by the air density (taken to be $1.225kg/m^3$) as we used the kinematic pressure in our solver.

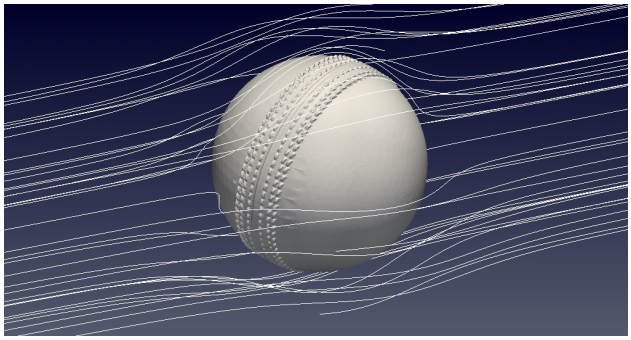

Figure 9: Streamlines for the solution of the potential flow problem. This serves as our initial condition for when we run simpleFoam.

We then used the potentialFoam command to solve the potential flow problem given these conditions which we then used this solution as a refined set of initial conditions for the flow.

Potential foam solves the continuity of mass equation $\nabla \cdot U = 0$ and the pressure equation $\nabla^2 p = 0$ and resultantly generates simplistic yet observationally plausible time zero conditions for simulation.

### 3.6 Limitations of the model

This model aims to be representative of the real world effects but there are many inherent flaws and assumptions made which alter the accuracy of our solution.

All fluid dynamics simulations must have a trade-off between the resolution of the mesh and the speed of computation. In this example, we are having to form a mesh fine enough to model the effects that each stitch in the seam may have upon the air. This again takes a long time to compute and a compromise has to be made as to how fine this mesh is. In the end we used a model with approximately 425,000 points defining 510,000 cells which was generated in approximately 30 minutes which we believe to be fine enough to capture the majority of the seam-air interaction.

In our model, we model the flight of the ball as though it remains at the same orientation as it moves through the air. However, this isn't the case during gameplay; we have mentioned earlier how the required bowling action in cricket has a tendency to impart back spin on the ball. If we took the ball to be rotating we would have to recompute the mesh at each and every time step, since a change in position of the ball relative to the air flow will have some aerodynamic effect. We also assume that the ball maintains orientation as it moves through the air. If this wasn't the case then we would again have to compute the mesh at each time step as well as working out any moments due to pressure disparity across the ball in order to work out how much rotation occurs at each time step. Recomputing the mesh is a very labour intensive process and would require more computing power than is feasibly available.

It is also well noted in cricket that if the team bowling polishes one side of the ball and leaves the other side to become roughened up during play we get to a point where one side of the ball moves through the air a lot more smoothly than the rough side. Thus more turbulent air flow is induced on one side than the other affecting the pressure difference and thus generating more swing. In our model, both sides of the ball are considered to behave identically in the air. We used a "noSlip" condition on the ball which defines the velocity to be 0 on the surface of the ball. This allows for the near surface pressure to be mapped accurately onto the balls surface and allows for simpler post processing as we can easily integrate pressure values on the surface to obtain the force acting on the ball. It is however, unrealistic to a degree and doesn't allow us to include any mention of surface roughness. From a cricketing standpoint, this means that our model will most accurately predict the air flow around a new ball and may not be as accurate once the ball becomes roughened due to play.

## 4 Analysis

### 4.1 Computation info

Initially, calculations were planned to be carried out on the University of Bristol's CREAM Linux cluster. With which I would have been able to carry out the simulations on 12*2.6GHz Intel Xeon cores with 48GB RAM. However, due to issues installing the OpenFOAM software on the cluster I had to resort to using a personal laptop to perform the computations.

Calculations were thus carried out on a more limited machine with 2*2.6GHz Intel i5-3230M cores with 8GB of RAM, with each of the 2 cores also possessing an extra logical core. Due to the reduction in available computational resources the ambition and detail of the simulations had to be scaled back accordingly.

Thus as mentioned previously, the generated mesh for each ball contained around 425,000 points and took

about 30 minutes to generate.

In running the solver, calculations were carried out in 0.001-second intervals for 0.5 seconds. With the results being recorded every 0.01 seconds. This choice of time steps meant that the simulations ran for approximately 50 minutes each, and meant that the resulting data set was a manageable 2GB for each run.

### 4.2 Post Processing Method

The entirety of a post processing relied on the Paraview software, a data visualisation and analysing software which is well suited to viewing the results of CFD simulations. Our main focus was to calculate the horizontal force that acts upon the ball. To this aim, we used the Paraview command "Extract Block" to isolate the surface of the ball for measurement. Next, we used "Generate Surface Normals" to define a unit normal vector for each and every cell surface on the ball. Care must be taken here, We must specify a no-splitting condition. This enforces that on sharp edges of the geometry that the cell isn't split and separate multiple normals are generated as this would affect the upcoming numerical integration.

We were then able to use the built-in calculator to find the effect of the pressure on each surface when looking in the x-direction, equivalent to the direction we expect the swing to occur. We found this by calculating $Normal_x \times (p \times 1.225 + 101325)$ for all of the approximately 72,000 cell surfaces on the ball. Here the dynamic pressure has been converted to actual pressure and then scaled by 1atm so that it is comparable to real world measurements. We were then able to perform a numerical surface integral across the ball which will give us the force in the positive x direction.

Due to the nature of a fluid dynamic simulation and with the inclusion of a turbulence model it is expected that this force will fluctuate for each time step. Thus we plot this resultant force for each saved time step and take the mean value of this a representative as the mean lateral force on the ball whilst it is in the air. A sample force-time plot can be seen below.

## 5 Varying the seam angle

We have explained earlier how the angle the seam makes to the incoming airflow underpins the mechanism behind swing. We hypothesise that there is a critical angle or region that serves to maximise the force produced. Intuitively we expect a ball with a seam angle of 0 or 90 not to produce any swing due to the scenario being symmetrical.

We also make note of the biomechanics of a fast bowlers action, it is most natural to bowl a ball with a seam angle of 0 and by the gentle angling of the wrist we would expect to achieve a range of up to around 45 degrees in either direction. In practice, it is very difficult to achieve seam angles at the upper end of this limit and still maintain control of the ball upon release and thus we shall concentrate on a smaller range of angles.

We created 11 variations of our ball geometry, in each case the seam-airflow angle was increased by intervals of 5 degrees up to a maximum of 50. We then ran the experiments in an identical set up with the wind speed set to $36ms^{-1}$ (80mph).

The horizontal force was calculated by the method outlined earlier, we then calculated this value for each time step of the simulation. The complete results of this are included at the end.

| | 0° | 5° | 10° | 15° | 20° | 25° | 30° | 35° | 40° | 45° | 50° |
|---|---|---|---|---|---|---|---|---|---|---|---|
| $\mu$ | 0.0520 | -0.1049 | -0.2257 | -0.2545 | -0.3036 | -0.2855 | -0.1776 | -0.2548 | -0.2815 | -0.2077 | -0.2095 |
| $\sigma$ | 0.0946 | 0.1487 | 0.1604 | 0.1528 | 0.1925 | 0.2153 | 0.2242 | 0.2838 | 0.3193 | 0.3835 | 0.5070 |

Table 1: Average Horizontal Force for varying Seam Angles

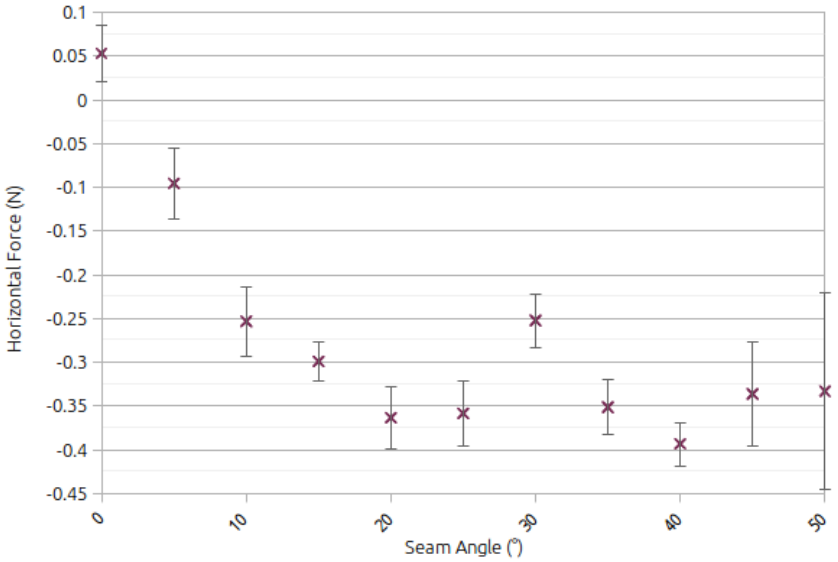


Figure 11: The average post-0.093s horizontal force plotted for each seam angle, error bars indicate $\pm 1.96 \times SE$

## 5.1 Analysis and comments

Overall these results support many of the current theories about swing bowling. We see clearly that initially, as we increase the seam angle that the force generated increases. Due to the symmetry of the set up, we would expect the 0° ball to generate no significant force in either direction and a mean force of 0.0520N supports this to an extent. We re-ran the simulation in this case but for 1.5 seconds instead of 0.5 seconds and obtained an average post-0.1s horizontal force of 0.0366N which gives further evidence to the validity of our expectation. The results of this are shown in figure 12 . Then we see the magnitude of the force generated increase steadily with seam angle until it reaches a value of 20° where the force seems to plateau between values of -0.4N and -0.3N. There is one exception to this, the ball with a seam angle of 30° has a slightly smaller force generated. Retrials were carried out in this scenario generating comparable results. but no explanation

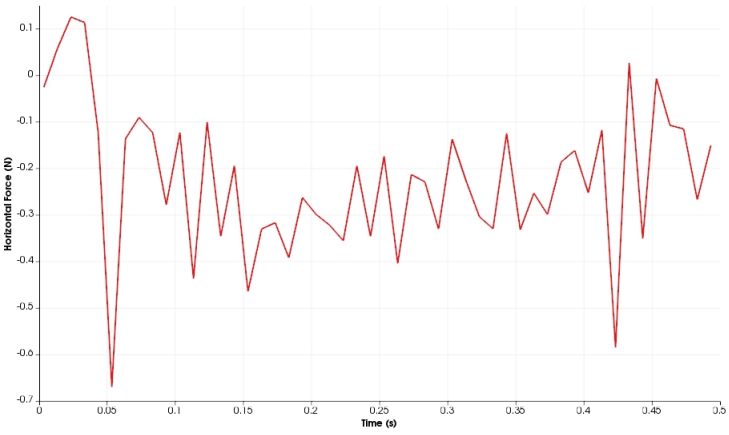


Figure 10: Horizontal force over time plot for the 10° ball at $36ms^{-1}$, highlighting the extent of fluctuations in force over time

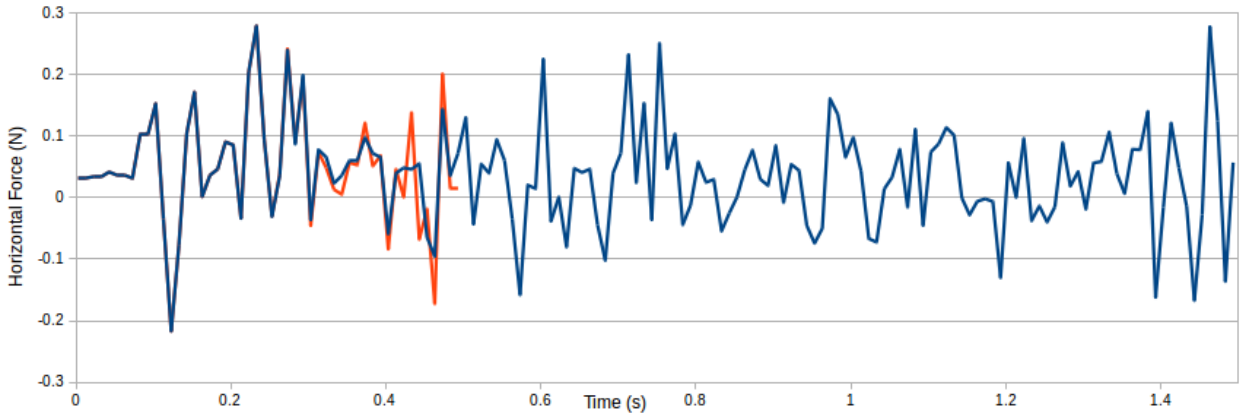


Figure 12: The horizontal force plotted against time for the 0° ball. The red line represents the original 0.5-second simulation while the blue line represents the 1.5-second simulation

can be offered at this time to explain this anomaly beyond attributing it to unfavourable fluctuations due to the recording times.

The exact method for calculating the predicted swing displacement will be explained in detail in a later section, but at this point it is worth calculating some rough values for the swing displacement at the stumps to demonstrate that this predicted force is plausible. For the 25° ball released horizontally from a height of 2m at $36ms^{-1}$ and thus experiencing approximately 0.35N of force at release. We would predict to have a displacement of around 31cm away from it's expected 'no-swing' displacement by the time it reaches the stumps. This is certainly within the realms observed in game play, and thus offers some confirmation as to the validity of our model.

For all the seam angles we see a common pattern emerge in the first 0.1 seconds of the simulation. Observe a typical result shown in figure 10. Initially, the force is acting in the positive x-direction and grows until roughly 0.033 seconds before then decreases until it takes on negative values and becomes more stable after approximately 0.1 seconds. We observe such features in the graphs for all tested seam angles which would be suggestive of initially the ball swings in the opposite direction expected. However, this result is most likely due to how we set up our initial velocity field. At time 0, we defined the velocity to be exactly $36ms^{-1}$ at every point in our mesh and then used the simplistic potentialFoam command to solve the potential flow in the set up which was then used to define the initial conditions. This is not concurrent with what we'd expect at the moment of release for a real cricket ball. In a bowler's delivery stride, the ball is accelerated up to its release speed causing considerable turbulence and a wake to form in the areas immediately behind the ball and hand. Thus our model assuming idealised flow around the ball in the domain is not accurate in that regard. The resultant early force is as a result of the system settling from this state into a more stable situation where the ball has a more chaotic wake forming behind it. Thus I believe we will obtain a better understanding of how seam angle affects the horizontal force if we exclude all the time steps up to and including 0.093s. A chart for this updated mean is included in figure 11.

We can also qualitatively examine how the wake forms and the similarities this has to the results from practical experiments. Examining figure 13, which is typical of results found for all late time steps for the 30° ball and above. We see that we do get a prominent wake as predicted however there are some subtleties that can be considered. The diagrams here show slices of the domain coloured according to the magnitude of the air velocity at that point.

If we look at the top down view of the ball we see that the flow separation occurs at an earlier point on the seam side of the ball than on the non-seam side, and as a result, the resulting wake is angled slightly to the right (positive x direction) as expected. We also see two distinct areas where the air velocity has lower magnitude. A similar observation may be made of the side on view of the ball as well, with two distinct zones at the top and bottom of the ball seemingly generating separate independent wakes.

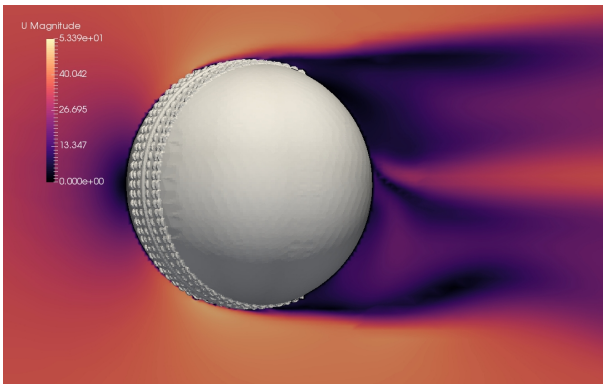


(a) A side on (Y-Z plane) view of the 30°ball.

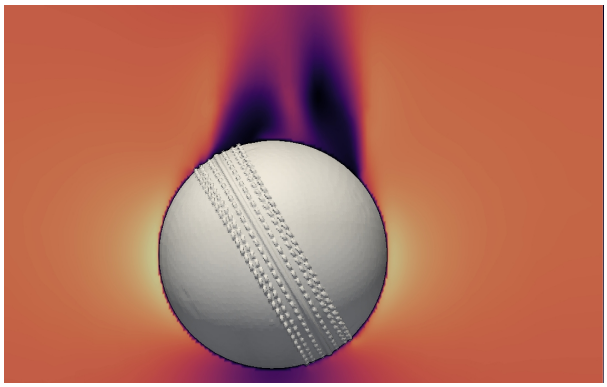

(b) A top down view (Y-Z plane) of the 30°ball from slice, 0.05cm above the equator

Figure 13: Example wakes formed by the 30° ball after approximately 0.4s.

An illustrative diagram explaining the behaviour of the air flow is given in the 3D contour plot in figure 14. Here we have plotted a contour for all points with a kinetic turbulent energy, k, greater than $4m^2s^{-2}$. This contour corresponds to areas where there is a less than negligible turbulence energy in the air it thus serves to show where any turbulent boundary layers have formed next to the ball's surface and suggests roughly where they separate from the surface. It is necessary to say that this value of $4m^2s^{-2}$ is contrived in order to produce clear diagrams, lowering the threshold causes nearly all the air close to the ball to be highlighted while raising the threshold result in only the wake being displayed. We also hypothesise that any adjustment in our initial k and $\omega$ values will affect this although no experiments have since been performed to determine the influence of changing these initial conditions. This means that although we can make general statements about the boundary layers we can't make any conclusive rulings as to their nature.

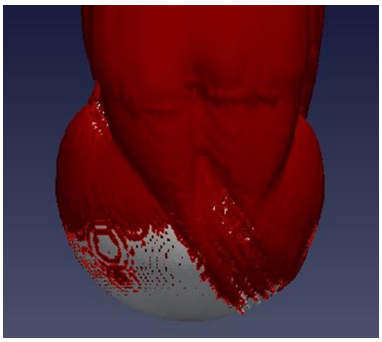

(a) A top down view (Y-Z plane)

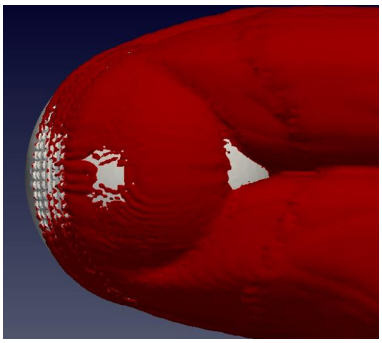

(b) Seam-side

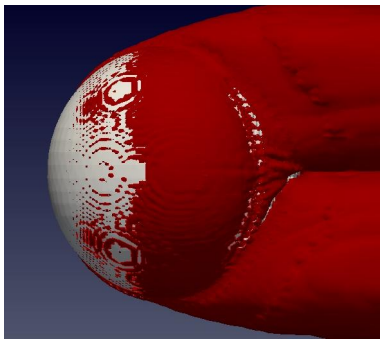

(c) The non-seam side

Figure 14: Contour plots for regions with turbulent kinetic energy greater than $4m^2s^{-2}$ for the 35 ° ball travelling at $36ms^{-1}$ (81 mph)

Looking at figure 14. The most noticeable feature is the extent and shape of the turbulent wake area. This evolves and spreads out behind the ball as predicted. Interestingly there exists a furrow that spreads from the equator and extends for at least 10cm behind the ball. This is almost perfectly mirrored on both the seam and non-seam side of the ball. On either side there typically exists a triangular area on the ball where there is no turbulent air present, although this occasionally appears and disappears with time and figure 14 doesn't show a time step where this is observed on the non-seam side. We predict this feature, perhaps showing a turbulent reattachment point at the rear of the ball is the cause of the aforementioned channel. This will potentially give rise to some issues as discussed later in this section.

As mentioned earlier, the current belief is that the angling of the seam causes the air to be tripped into a turbulent boundary layer on one side of the ball. Our results generally back this theory up. On the seam side, the turbulent layer forms slightly behind the seam and on the halfway point for the non-seam side. However; the crucial detail here is happening on the seam itself on the top and bottom of the ball. We see that along the whole length of the seam there is turbulent air in its immediate wake. Yet near the equator of the ball this appears to quickly reattach whereas near the top and bottom of the ball this layer grows and quickly develops into the main wake. This is in agreement with the current theory behind swing although our model places more importance on the airflow near the top and bottom of the ball rather than evenly spread over the length of the seam as some explanations suggest.

A clearer image can be generated by looking at a simpler model of the ball and can be seen in figure 15. We produced a sphere of identical size as the accurate model, but instead of a detailed seam, we intersect a cylinder with a height of 1cm which extrudes 3mm from the ball surface. Repeating the same analysis with the ball angled at 20° to airflow. Here the seam clearly generates a turbulent boundary layer across its entire length on the seam side of the ball, whereas on the non-seam side we again observe the layer forming halfway across the ball.

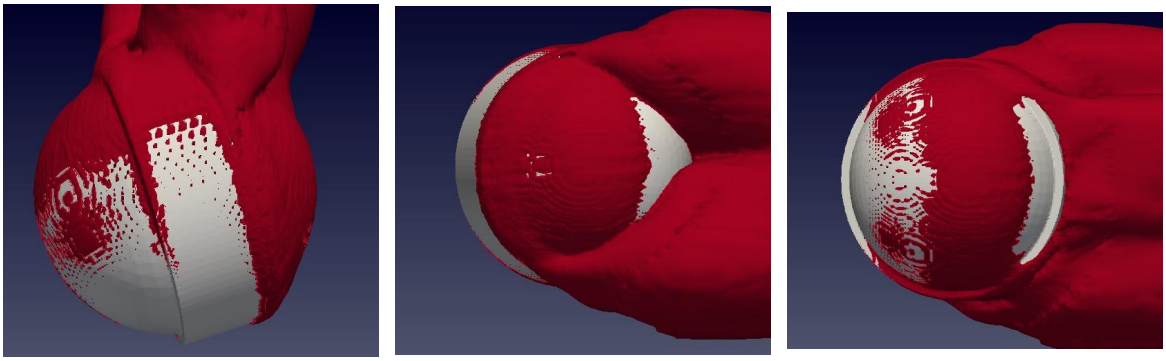

(a) A top-down view (Y-Z plane) (b) Seam side (c) The non-seam side)

Figure 15: Contour plots for regions with turbulent kinetic energy greater than $4m^2s^{-2}$ for a simplified ball angled at 20° to air travelling at $36ms^{-1}$ (81 mph)

There is a comment to make on the physical experiments done at this point. The K. Bentley and Mehta. (1982) work which is referenced along with Barton (1982) in R. D. Mehta (1985) review as being the foundation the experimental evidence for swing. In these experiments Bentley et al examined the pressure by installing small pressure sensors around the equator of the ball. Thus they were able to plot the pressure around the circumference and infer from this the optimal angles to maximise swing displacement. However, our model suggests that at the equator of the ball we get some unusual results which may not be indicative

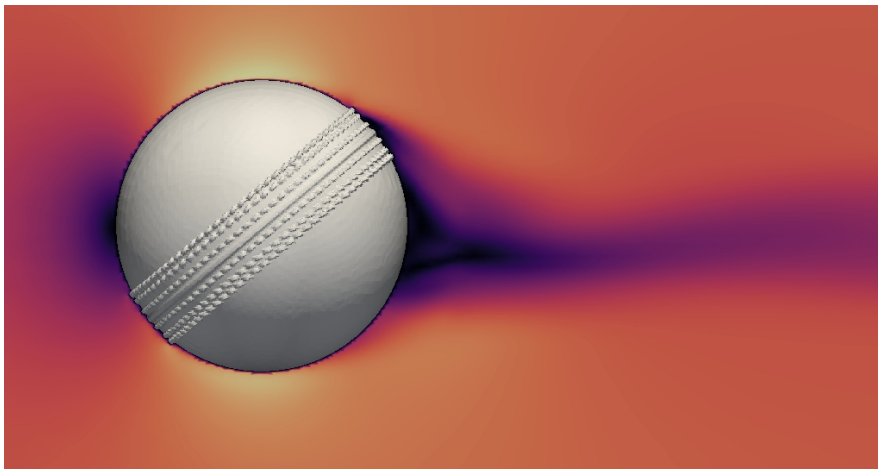

Figure 16: Top down view of the wake of the 40° ball at $31ms^{-1}$ after 0.48s

of the overall situation. Figure 16 shows the flow along a slice through the equator, it is noticeably smaller than the off centred top down wake seen in figure 13. Thus while taking pressure tappings may be sufficient to show comparisons between different seam angles, it is unlikely to provide accurate data from which to calculate the resultant forces.

# 6 Varying the release speed

Both players and writers on the game are in agreement with the notion that there is an optimal speed at which to bowl to generate threatening swing. A cohort of 'military' medium pace bowlers exist in the English professional game that attests to this. This is backed up by wind tunnel experimentation performed in K. Bentley and Mehta. (1982) and Barton (1982), whose results are aptly stated by R. Mehta (2014) that "The maximum side force is obtained at a bowling speed of about 30 m/s (67 mph) with the seam angled at 20° and the ball spinning backwards at a rate of 11.4 revs/s". The same Rabi Mehta goes as far to state in an albeit journalistic article that as we increase the ball speed from 70mph that "the asymmetry is reduced and so is the swing such that at around 80 mph there is no swing." R. Mehta (2006b).

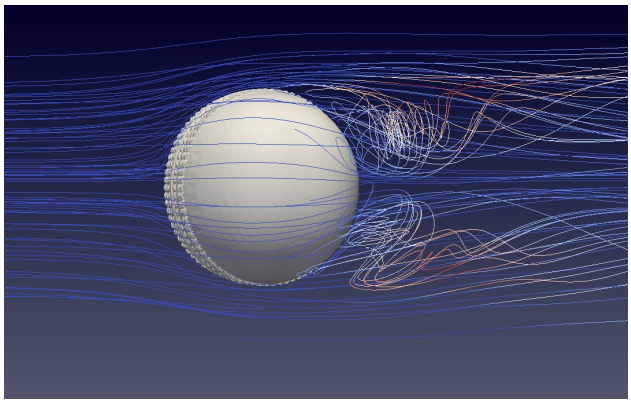

Figure 17: Streamlines of the air flow around the 30° ball. Note the two distinct wake vortices forming at the top and bottom. Streamlines are coloured according to their turbulent kinetic energy

We thus highlighted an illustrative selection of seam angles for which we attained lateral forces and ran those simulations again but over a variety of speeds to see if our model backs up these claims. The speeds chosen were distributed from $26ms^{-1}$ up to a maximum of $43ms^{-1}$ (58 mph to 96 mph) where the upper end of the scale accounts for some of the consistently fastest bowlers in the professional game while the lower end covers bowling speeds commonly seen by amateur fast bowlers (see Cork, Justham, and West (2013)).

The angles 10° 20° and 40° were chosen. The 10° ball marked highest angle before which the force appears to stabilise between 0.3N and 0.4N. Where as the 25° ball and 40° ball both covered a convenient range and generated 2 of the 3 largest lateral forces observed.

Once again, we see similar patterns for the force generated in the first 0.1 seconds of the simulation. Thus we exclude these values and instead give the mean and standard deviation for the post 0.1-second forces.

| | | Release Velocity (m/s) | | | | | | | | |
|---|---|---|---|---|---|---|---|---|---|---|
| | | 26 | 29 | 31 | 34 | 36 | 38 | 40 | 41.5 | 43 |
| 10° | $\mu$ | -0.1119 | -0.1425 | -0.1606 | -0.2035 | -0.2533 | -0.2352 | -0.2757 | -0.3245 | -0.3608 |
| | $\sigma$ | 0.0430 | 0.0828 | 0.0816 | 0.1204 | 0.1261 | 0.1499 | 0.1081 | 0.1801 | 0.1316 |
| 25° | $\mu$ | -0.1963 | -0.2315 | -0.2665 | -0.3109 | -0.3584 | -0.4038 | -0.3773 | -0.4216 | -0.4777 |
| | $\sigma$ | 0.0469 | 0.0808 | 0.0552 | 0.0999 | 0.1190 | 0.0977 | 0.1250 | 0.1608 | 0.1564 |
| 40° | $\mu$ | -0.2202 | -0.2563 | -0.2989 | -0.3597 | -0.3933 | -0.4620 | -0.5015 | -0.5308 | -0.5447 |
| | $\sigma$ | 0.0355 | 0.0661 | 0.0587 | 0.0641 | 0.0786 | 0.0663 | 0.1092 | 0.0998 | 0.1045 |

Table 2: Average horizontal force for 3 seam angles released at varying velocities

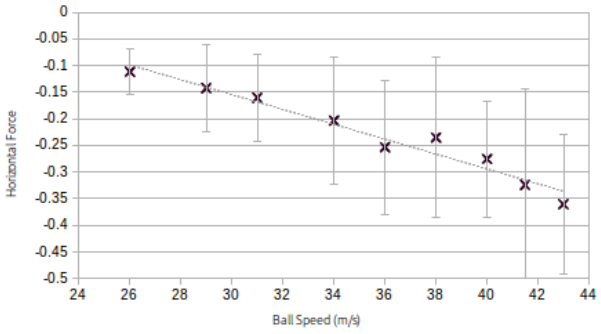


(a) 10°

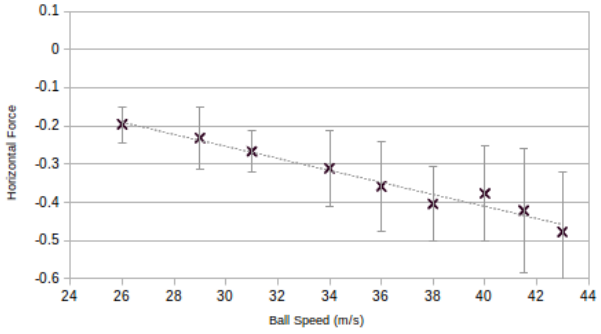


(b) 25°

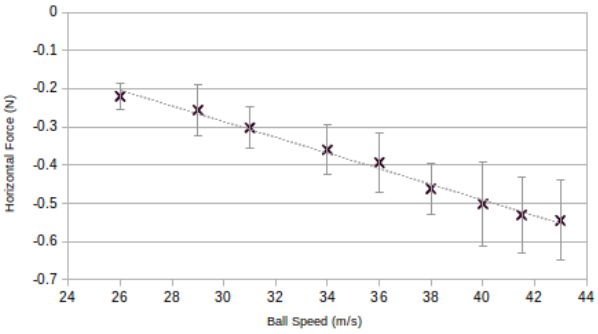


Figure 19: 40°

Figure 20: Force - Velocity graphs for the 10° 25° and 40° balls with Linear trend lines added. Y error lines mark SD. Trend lines possess $R^2$ values of 0.955, 0.964 and 0.991 respectively.

### 6.1 Analysis and comments

The immediate observation, in this case, is that there appears to be a linear relationship between the release velocity and the average force generated for all tested seam angles, This is backed up by our high coefficient of determination values. And although we have only sampled 9 release velocities in each scenario, the fact this relationship is observed across all seam angles adds weight to its credibility.

This result is also curious in that it defies the purported notion that there is an optimal sweet spot that medium-fast bowlers (approx 33-36 $ms^{-1}$) utilise to generate the maximum swing. There are a few reasons why this disconnect between experiment and observed bowling strategy might exist. Firstly, we must consider how swing bowling threatens the batsman. This is usually by either having an out-swinging delivery catch the bat's edge as a shot is played and providing a simple catch to the wicket-keeper, slips, or a close fielder. Or by an in-swinging delivery targeting the bowled and LBW dismissals. Both of these methods require the bowler to be resolute in his seam position and accurate in where they intend to bowl the ball. There's anecdotal evidence to suggest that many bowlers overexert themselves in order to bowl faster and do so at the expense of their accuracy but the author knows no experiments connecting bowling speed to accuracy. This may explain the difference in observed strategies. However, it still remains difficult to reconcile our model against results obtained in the previously mentioned studies.

There is another factor we must consider when examining whether we see faster bowlers generate more swing. In this case there is a trade-off to be considered. Our model predicts that a ball travelling faster through the air will generate a greater lateral force than a slower ball. This doesn't necessarily correlate to a greater swing displacement by the time the ball reaches the batsman. A faster ball will spend less time in the air and thus may not have as much time to swing. This relationship is further complicated as a bowler alters the balls release angle relative to the horizontal. Thus in the next section, we create a model that will estimate the ball's trajectory to examine if there is an optimal bowling speed to generate the greatest swing displacement for a fixed seam angle. Despite this, we hypothesise that due to the horizontal force being linear with velocity and the time in the air being linear if we exclude the effect of drag that the overall swing displacement will be approximately constant.

## 7 Predicting Trajectories

Using the same method we used to calculate the horizontal force that acted in the x direction, we can also calculate the drag force that acts in the y direction. Then using the relationship defined earlier

$$F_{drag} = \frac{1}{2}\rho U^2 C_d \pi r^2$$

Using the same technique we used to find the swing force we can find the drag force and thus calculate the drag coefficient for the variously angled balls.

Alam et al. (2010) performed wind tunnel experiments on the side force and drag coefficient for new and used cricket balls. Concluding that cricket balls exhibit "significant" differences to smooth spheres; cricket balls don't exhibit a rapid reduction in drag at critical Reynold numbers. The measurements for a new ball are included below.

In our simulations we have considered velocities from $26ms^{-1}$ to $42ms^{-1}$ which correspond to Reynold numbers between $1.1 \times 10^5$ and $1.8 \times 10^5$. Alam et al measured the drag coefficient for the $40^\circ$ ball to be between 0.45 and 0.55 for the majority of our values increasing to 0.6 at the very lower end of our range. Our

results agree observationally with these values, with the drag coefficient for our 40° ball at $29ms^{-1}$ calculated to be 0.48.

For simplicity, we will use this value as an approximate value for our trajectory prediction in for all angled balls at all speeds.

Coupling this value with the linear relationship we obtained between swing force and velocity we are able to calculate trajectories the ball follows. A model that will take into account how drag affects the ball and how the swing force varies as a result.

We must first make a few assumptions to simplify the model. Although we are accounting for drag in the y-direction down the pitch we will not account for it in the x and z directions as the corresponding velocities generate negligible drag.

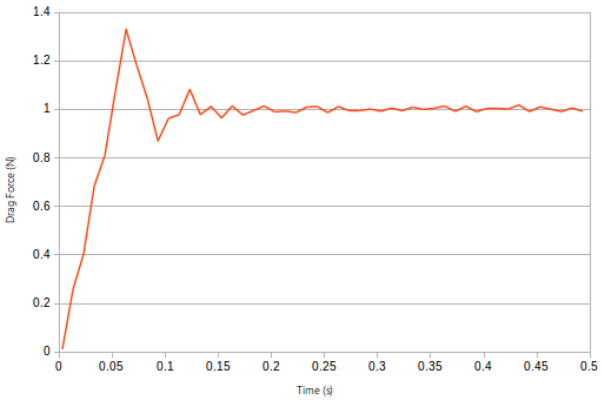


Figure 21: The Drag force over time graph for the 40° ball at $29ms^{-1}$. Note how we again get unusual behaviour in the first 0.1 seconds before stability is reached around a drag force of 1N

We will also assume that the bowler releases the ball directly above the crease. This means that the ball needs to travel a displacement of 18.9m down the pitch to reach the other set of stumps. We also do not model for any initial lateral velocity on the ball. This assumes that the ball initially travels parallel to the pitch and thus all lateral displacement will be due to swing. Computationally, neither of these two conditions would be hard to implement into the code, the first assumption merely reduces the need for an extra input parameter. The second assumption though can cause some issues; if we do account for initial lateral velocity then this will influence the angle the seam makes with the oncoming air. This could easily invalidate our calculations for the swing if it were too high, it would require considerable work to implement this correction and would require a larger sample set of seam angles in order to provide a reputable insight.

We will also track the swing displacement of the ball until it bounces then we make the assumption that it will carry on with its current x-velocity and will not swing any more after it has bounced. This is a reasonable assumption since bouncing often imparts rotations on the ball that will mean that we now have a rapidly varying seam angle and thus don't develop the symptomatic asymmetric wake. In real life, Bowlers look to create uneven vertical and lateral bounce by how they position the seam, this will affect the direction of the post-bounce velocity and is not accounted for in the model.

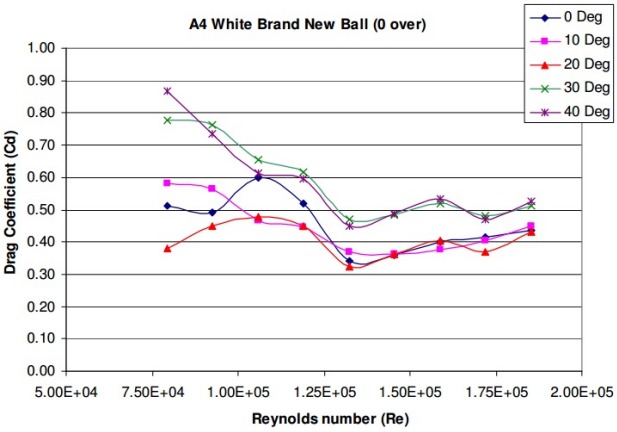


Figure 22: Measured drag force coefficients for a new cricket ball source: Alam et al. (2010)

We use numeric methods to obtain solutions for the horizontal displacement. We calculate the y-velocity of the ball every 0.001s and how it changes due to the drag force. Then for each y-velocity, we use our linear relationship between release speed and lateral force to find the force that acts in the x direction.

For each time step we can then work out the displacement moved in the x direction from release at each particular instant.

We then can calculate at which time step the ball bounces, and then, by a series of IF constraints, switch our model to that of a standard particle with initial conditions defined by the values at the bounce time. By combining these two models we can then obtain an overall value for the swing displacement from it's expected trajectory at the instance the ball passes the stumps.

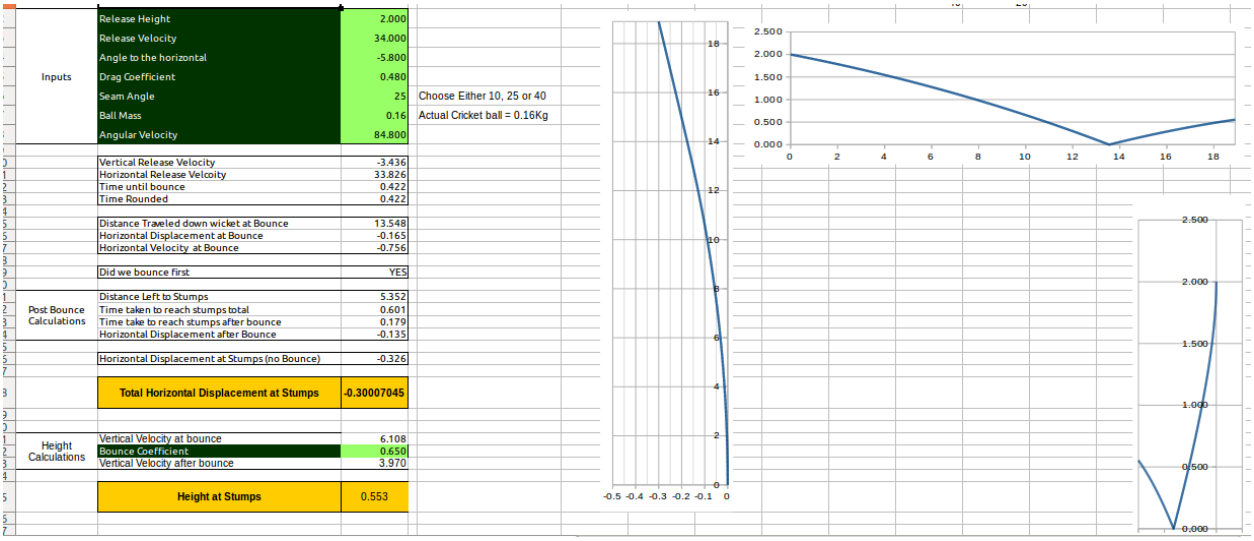


Figure 23: A screen capture of the trajectory predictor

One notion that this model gives an explanation for is the idea of 'late swing'. This has been described by cricket enthusiasts as balls that appear to swing considerably just before reaching the batsman. If we take an example of a ball bowled at $34ms^{-1}$ that first bounces 13.5m down the pitch. In this instance we calculate a swing displacement of 30.0cm by the time the ball reaches the stumps; however, if we then look up the point where the displacement reaches 15cm we see that this occurs after 0.405 seconds when the ball has travelled 12.97m down the wicket. That is the ball travels 50% of its total swing displacement in the final 32% of its path down the pitch. Thus appearing to move late on in its journey.

We investigate the claim that swing displacement varies with release velocity by adjusting the bowling speed and the release angle such that the ball pitches either at a good length (13.5m down the wicket) or on a yorker length (at the base of the stumps). We chose the angle to 1dp such that the ball first bounces closest to either 13.5m or 18.9m. The yorker delivery allows for maximum swing displacements for a given speed under our assumptions whereas the good length ball is intended to be typical of a length bowled in a game and thus allows for comparisons to be made.

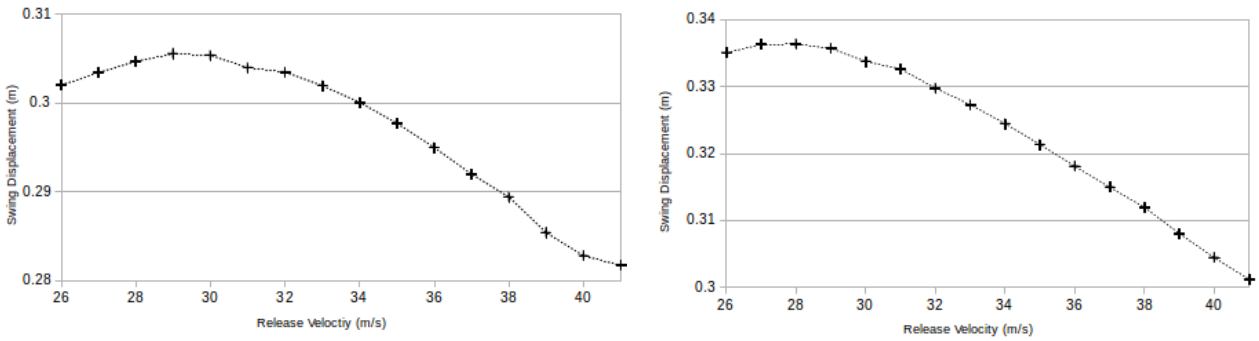


(a) Good Length

(b) Yorker Length

Figure 24: Absolute value of the swing displacement for varying release velocities for the 25° ball

Our results do unexpectedly show optimal bowling speeds to maximise the swing displacement at 29 and $28ms^{-1}$ respectively. But the corresponding difference between overall swing displacement varies in a range of 2.5cm and 3.5cm in each case. These are not significant enough to demonstrate that bowling at around $29ms^{-1}$ is the optimal sweet spot we have mentioned previously. Instead it is my belief that the real game effectiveness of swing bowling may not be solely dependent upon displacement achieved and instead that there may be an optimal range of displacements such that the ball moves enough as to deceive the batsman and catch the edge of the bat; but not too much that the batsman misses the ball entirely.

# 8 Conclusions and Recommendations

The results have demonstrated that our CFD solution gives evidence to the theory of conventional swing as first proposed by Cooke (1955). We have shown how the seam angle affects the boundary layer separation point and that this leads to a correlation between the angle of the seam relative to the airflow and the lateral force generated. Our results showed that the force increases up to a critical angle of about 20° . We have also given evidence to a linear relationship between lateral force and bowling speed.

In our spreadsheet-based trajectory projector, we have used our results to predict firstly the forces and thus the resulting motion of the ball ultimately giving us the 'swing' displacement. We obtained values up to a maximum of around 35cm for elite level bowlers a figure which is in the range of match observed values.

It is hoped that the model and subsequent results are able to add insight to the fluid behaviour present in conventional swing. And that by comparing results with other forays into CFD simulations of swing such as those by Penrose, Hose, and Trowbridge (1996); Latchman and Pooransingh (n.d.) and Pahinkar and Srinivasan (2010) which have begun to provide a computational explanation for swing.

Simple refinements to this model and the reliability of our simulation may be made by increasing the resolution of our mesh and by rerunning scenarios to observe the effect, if any, of turbulence on the swing. It is predicted that in order to gain a much more accurate model we would have to incorporate backspin on the ball, both along the axis of the seam and when the seam has a more commonly observed 'wobble'. However, the computational power required in this instance lies beyond that of personal computers and would more likely entail high-performance computers running for several days to obtain the required data.

Further improvements may be had in adjusting the time steps used in our calculations. We measured

at 0.001s intervals, however when we compare the speeds simulated in comparison to the scale of the seam on a cricket ball it is apparent that even a 0.001s time step may be insufficient. This again would only be viable with further computing power and in this instance the effect would not likely be significant enough to meaningfully alter our results.

We also took some liabilities with calculating values for the drag coefficient. With our model, it would be possible to perform direct calculations for the drag coefficient for all balls and tested velocities and provide a more in depth analysis between these values and those obtained by Alam et al. (2010). However the results of refining the drag coefficient values would only have a minor influence on our prediction model but would serve to offer further evidence as to the credibility of our model.

# 9 Appendix: tables of results

Table 3: Horizontal force for differing seam angles at each time step (Velocity - $36ms^{-1}$)

| Time | 0° | 5° | 10° | 15° | 20° | 25° | 30° | 35° | 40° | 45° | 50° |
|---|---|---|---|---|---|---|---|---|---|---|---|
| 0.003 | 0.031716 | -0.033128 | -0.025536 | -0.013026 | -0.034216 | -0.04696 | 0.028052 | -0.017353 | -0.03669 | 0.035999 | 0.027342 |
| 0.013 | 0.031227 | 0.0081276 | 0.058092 | 0.11413 | 0.13432 | 0.16402 | 0.2752 | 0.26675 | 0.27766 | 0.36611 | 0.3646 |
| 0.023 | 0.033449 | 0.039321 | 0.1263 | 0.22874 | 0.31135 | 0.40595 | 0.58295 | 0.64542 | 0.71765 | 0.84925 | 0.87018 |
| 0.033 | 0.034667 | 0.046356 | 0.11423 | 0.22345 | 0.31917 | 0.4585 | 0.68294 | 0.84614 | 0.97776 | 1.2211 | 1.4142 |
| 0.043 | 0.041945 | -0.11001 | -0.12395 | -0.024035 | 0.023224 | 0.088191 | 0.35144 | 0.49097 | 0.63547 | 0.80413 | 0.95298 |
| 0.053 | 0.036165 | -0.65188 | -0.67217 | -0.51542 | -0.3788 | -0.31319 | -0.078756 | 0.24337 | 0.34365 | 0.51448 | 0.39826 |
| 0.063 | 0.035714 | -0.13143 | -0.13662 | -0.41598 | -0.39892 | -0.17191 | -0.14555 | -0.17281 | -0.11683 | -0.075372 | -0.22095 |
| 0.073 | 0.031735 | -0.033304 | -0.09044 | -0.10703 | -0.14406 | -0.27594 | -0.26027 | -0.29504 | -0.40179 | -0.20443 | -0.53653 |
| 0.083 | 0.10366 | -0.25989 | -0.12334 | -0.13473 | -0.27123 | -0.20316 | -0.14772 | -0.41419 | -0.44051 | -0.1772 | -0.89911 |
| 0.093 | 0.104 | -0.30338 | -0.27898 | -0.11751 | -0.20536 | -0.047811 | -0.082792 | -0.28375 | -0.30054 | -0.26974 | 0.47832 |
| 0.103 | 0.15308 | -0.18531 | -0.12261 | -0.32204 | -0.59871 | -0.10774 | -0.19789 | -0.42879 | -0.42321 | -0.2932 | 0.018575 |
| 0.113 | -0.034848 | -0.23305 | -0.43832 | -0.1888 | -0.14742 | -0.27511 | -0.17384 | -0.54347 | -0.39814 | -0.3501 | -0.18136 |
| 0.123 | -0.21697 | -0.1408 | -0.10018 | -0.21923 | -0.44466 | -0.49549 | -0.38379 | -0.35198 | -0.41911 | -0.30841 | -0.055737 |
| 0.133 | -0.076672 | -0.20178 | -0.34691 | -0.27698 | -0.29098 | -0.36955 | -0.36203 | -0.2563 | -0.4888 | -0.43158 | -0.52416 |
| 0.143 | 0.10443 | -0.17153 | -0.19454 | -0.12941 | -0.38294 | -0.49293 | -0.31064 | -0.46486 | -0.5904 | -0.34834 | -0.29792 |
| 0.153 | 0.1718 | -0.31668 | -0.46574 | -0.31453 | -0.37598 | -0.43451 | -0.28932 | -0.49606 | -0.28693 | -0.34834 | -0.22821 |
| 0.163 | 0.0018454 | -0.16761 | -0.33119 | -0.26524 | -0.24597 | -0.45967 | -0.10815 | -0.36491 | -0.39473 | -0.42429 | -0.66159 |
| 0.173 | 0.036632 | -0.33214 | -0.31744 | -0.38643 | -0.49914 | -0.23127 | -0.22212 | -0.29772 | -0.39067 | -0.25154 | -0.054258 |
| 0.183 | 0.0467 | 0.14528 | -0.39321 | -0.19738 | -0.2228 | -0.40002 | -0.29622 | -0.32089 | -0.35639 | -0.36783 | -0.44372 |
| 0.193 | 0.090828 | -0.029111 | -0.26322 | -0.30074 | -0.52075 | -0.27825 | -0.22709 | -0.41433 | -0.44406 | -0.30992 | -0.65854 |
| 0.203 | 0.085925 | -0.026791 | -0.29951 | -0.41258 | -0.22914 | -0.28578 | -0.3367 | -0.24366 | -0.25779 | -0.26149 | 0.12837 |
| 0.213 | -0.03311 | 0.029318 | -0.32278 | -0.26985 | -0.30404 | -0.3637 | -0.26584 | -0.31038 | -0.4576 | -0.44669 | -0.70307 |
| 0.223 | 0.20409 | -0.21254 | -0.35631 | -0.39119 | -0.61565 | -0.37374 | -0.28832 | -0.21927 | -0.30402 | -0.20304 | -0.26573 |
| 0.233 | 0.27938 | -0.21392 | -0.19464 | -0.31674 | -0.2761 | -0.43578 | -0.17712 | -0.41915 | -0.38719 | -0.37608 | -0.13335 |
| 0.243 | 0.095 | -0.051332 | -0.34716 | -0.25904 | -0.4825 | -0.18305 | -0.13089 | -0.25466 | -0.48101 | -0.36214 | -0.81579 |
| 0.253 | -0.02984 | -0.1405 | -0.1739 | -0.37946 | -0.33226 | -0.47809 | -0.38085 | -0.42971 | -0.25173 | -0.18577 | 0.19721 |
| 0.263 | 0.038225 | -0.23582 | -0.40553 | -0.24857 | -0.29215 | -0.2748 | -0.18095 | -0.3231 | -0.52538 | -0.5075 | -0.61861 |
| 0.273 | 0.24205 | -0.15819 | -0.21366 | -0.33874 | -0.34254 | -0.35578 | -0.4117 | -0.32984 | -0.29505 | -0.20216 | -0.47858 |
| 0.283 | 0.091038 | -0.096408 | -0.22957 | -0.25972 | -0.38302 | -0.42213 | -0.1154 | -0.38755 | -0.38186 | -0.33852 | 0.085305 |
| 0.293 | 0.19235 | -0.11304 | -0.33105 | -0.26834 | -0.34259 | -0.15078 | -0.1852 | -0.21175 | -0.47266 | -0.4492 | -0.87416 |
| 0.303 | -0.045178 | -0.18416 | -0.13722 | -0.33378 | -0.43385 | -0.55297 | -0.34348 | -0.44839 | -0.25883 | -0.089925 | 0.056981 |
| 0.313 | 0.073889 | -0.21063 | -0.22529 | -0.30809 | -0.18344 | -0.11175 | -0.15903 | -0.21598 | -0.49683 | -0.55641 | -0.44021 |
| 0.323 | 0.048782 | -0.2021 | -0.30466 | -0.33103 | -0.45552 | -0.52884 | -0.3477 | -0.40932 | -0.32379 | -0.20553 | -0.68602 |
| 0.333 | 0.013388 | -0.088661 | -0.33049 | -0.31133 | -0.31819 | -0.21006 | -0.13887 | -0.35566 | -0.42268 | -0.27269 | 0.20866 |
| 0.343 | 0.005492 | 0.048162 | -0.1247 | -0.29574 | -0.36434 | -0.41562 | -0.19166 | -0.23473 | -0.3586 | -0.55229 | -0.83716 |
| 0.353 | 0.057162 | 0.12389 | -0.3327 | -0.41916 | -0.42029 | -0.46901 | -0.29241 | -0.51546 | -0.3776 | -0.015432 | -0.13108 |
| 0.363 | 0.053146 | -0.051207 | -0.25375 | -0.18889 | -0.2268 | -0.32984 | -0.29952 | -0.21908 | -0.40341 | -0.58997 | -0.24443 |
| 0.373 | 0.12163 | 0.060079 | -0.29972 | -0.34481 | -0.48698 | -0.34166 | -0.35376 | -0.44874 | -0.33275 | -0.23877 | -0.80837 |
| 0.383 | 0.051574 | -0.14769 | -0.18662 | -0.2945 | -0.22968 | -0.31218 | -0.065398 | -0.35403 | -0.4609 | -0.19689 | 0.22232 |
| 0.393 | 0.068372 | -0.19508 | -0.16178 | -0.31808 | -0.46502 | -0.53199 | -0.12079 | -0.27399 | -0.35773 | -0.63889 | -0.7464 |
| 0.403 | -0.083577 | 0.061657 | -0.25323 | -0.39785 | -0.35465 | -0.28624 | -0.42785 | -0.51733 | -0.43277 | 0.047649 | -0.29916 |
| 0.413 | 0.046148 | 0.095622 | -0.11744 | -0.22291 | -0.23499 | -0.48368 | -0.16113 | -0.20847 | -0.39303 | -0.59983 | -0.049505 |
| 0.423 | 0.0011896 | 0.042102 | -0.58692 | -0.39341 | -0.46025 | -0.18972 | -0.3328 | -0.43396 | -0.35179 | -0.27741 | -0.88836 |
| 0.433 | 0.13844 | 0.075759 | 0.027471 | -0.14932 | -0.29152 | -0.42759 | -0.2773 | -0.36549 | -0.45733 | -0.13865 | 0.15028 |
| 0.443 | -0.067644 | -0.23019 | -0.35185 | -0.39803 | -0.45738 | -0.39804 | -0.35099 | -0.23427 | -0.30776 | -0.69318 | -0.6043 |
| 0.453 | -0.018311 | -0.002644 | -0.0061283 | -0.29038 | -0.31775 | -0.26002 | -0.35228 | -0.48397 | -0.4499 | 0.071281 | -0.51035 |
| 0.463 | -0.17232 | 0.10829 | -0.10744 | -0.37625 | -0.30873 | -0.48794 | -0.10282 | -0.2539 | -0.40529 | -0.60074 | 0.13053 |
| 0.473 | 0.20129 | -0.096016 | -0.11515 | -0.22257 | -0.34235 | -0.29048 | -0.27231 | -0.3621 | -0.31489 | -0.30429 | -0.89117 |
| 0.483 | 0.014906 | 0.050664 | -0.26782 | -0.31831 | -0.50335 | -0.44371 | -0.24086 | -0.41073 | -0.49346 | -0.11546 | 0.0052165 |
| 0.493 | 0.16383 | -0.22272 | -0.1507 | -0.30651 | -0.34995 | -0.39552 | -0.21211 | -0.23586 | -0.32408 | -0.71657 | -0.39705 |

Table 4: Horizontal force for the 10° 25° and 40° balls for differing release velocities at each time step

| Time | 26 | 29 | 31 | 34 | 36 | 38 | 40 | 42 | 43 |
|---|---|---|---|---|---|---|---|---|---|
| 0.003 | -0.0255 | -0.0255 | -0.0255 | -0.0255 | -0.0255 | -0.0255 | -0.0255 | -0.025536 | -0.025536 |
| 0.013 | 0.0163 | 0.0272 | 0.0353 | 0.0485 | 0.0581 | 0.0682 | 0.0788 | 0.087196 | 0.095945 |
| 0.023 | 0.0521 | 0.0721 | 0.0867 | 0.1096 | 0.1263 | 0.1444 | 0.1636 | 0.1784 | 0.19388 |
| 0.033 | 0.0465 | 0.0641 | 0.0771 | 0.0983 | 0.1142 | 0.1300 | 0.1474 | 0.16059 | 0.17479 |
| 0.043 | -0.0970 | -0.1102 | -0.1173 | -0.1225 | -0.1240 | -0.1276 | -0.1238 | -0.11958 | -0.1183 |
| 0.053 | -0.3955 | -0.4680 | -0.5209 | -0.6108 | -0.6722 | -0.7372 | -0.8030 | -0.85122 | -0.89796 |
| 0.063 | -0.0568 | -0.0617 | -0.0750 | -0.1069 | -0.1366 | -0.1617 | -0.1898 | -0.20855 | -0.2267 |
| 0.073 | -0.0745 | -0.0610 | -0.0637 | -0.0775 | -0.0904 | -0.0986 | -0.1068 | -0.10557 | -0.10386 |
| 0.083 | -0.0988 | -0.0893 | -0.0954 | -0.1098 | -0.1233 | -0.1670 | -0.2156 | -0.21866 | -0.22932 |
| 0.093 | -0.1130 | -0.2049 | -0.1825 | -0.2308 | -0.2790 | -0.3473 | -0.4440 | -0.51078 | -0.55638 |
| 0.103 | -0.0884 | -0.1146 | -0.1469 | -0.1359 | -0.1226 | -0.1468 | -0.3120 | -0.36652 | -0.41769 |
| 0.113 | -0.0812 | -0.1467 | -0.2377 | -0.3761 | -0.4383 | -0.4078 | -0.3456 | -0.41572 | -0.45377 |
| 0.123 | -0.1340 | -0.1148 | -0.1462 | -0.2171 | -0.1002 | -0.0133 | -0.1474 | -0.27218 | -0.20439 |
| 0.133 | -0.1056 | -0.1411 | -0.1674 | -0.2639 | -0.3469 | -0.5044 | -0.3658 | -0.40837 | -0.46384 |
| 0.143 | -0.1441 | -0.1941 | -0.2049 | -0.1600 | -0.1945 | -0.4267 | -0.1807 | -0.1844 | -0.11196 |
| 0.153 | -0.0467 | -0.0307 | -0.1013 | 0.0409 | -0.4657 | -0.3151 | -0.4289 | -0.34237 | -0.44049 |
| 0.163 | -0.1353 | -0.3468 | -0.2712 | -0.3775 | -0.3312 | -0.2781 | -0.1919 | -0.21908 | -0.57656 |
| 0.173 | -0.0695 | -0.1995 | -0.1762 | -0.0674 | -0.3174 | -0.3754 | -0.2873 | -0.59656 | -0.48416 |
| 0.183 | -0.1035 | -0.2327 | -0.2957 | -0.3438 | -0.3932 | -0.2632 | -0.3036 | -0.42069 | -0.46147 |
| 0.193 | -0.1120 | -0.0605 | -0.2004 | -0.1698 | -0.2632 | -0.4244 | -0.2389 | -0.42049 | -0.13497 |
| 0.203 | -0.1028 | -0.1443 | -0.2149 | -0.3323 | -0.2995 | -0.3011 | -0.5965 | -0.18999 | -0.23711 |
| 0.213 | -0.0966 | -0.1720 | -0.0646 | -0.4493 | -0.3228 | -0.2188 | -0.2815 | -0.31766 | -0.63505 |
| 0.223 | -0.0681 | -0.0231 | -0.1329 | -0.1651 | -0.3563 | -0.4395 | -0.4122 | -0.39893 | -0.62208 |
| 0.233 | -0.1125 | -0.2243 | -0.0234 | -0.2120 | -0.1946 | -0.2486 | -0.2359 | -0.34679 | -0.30568 |
| 0.243 | -0.1946 | -0.1600 | -0.2381 | -0.1670 | -0.3472 | -0.3714 | -0.3426 | -0.60537 | -0.22742 |
| 0.253 | -0.1627 | -0.0929 | -0.1263 | -0.1698 | -0.1739 | -0.0183 | -0.2124 | 0.072652 | -0.38427 |
| 0.263 | -0.1812 | -0.1037 | -0.0834 | -0.3255 | -0.4055 | -0.1925 | -0.4400 | -0.56243 | -0.21291 |
| 0.273 | -0.1337 | -0.1523 | -0.0787 | -0.0791 | -0.2137 | -0.1681 | -0.2875 | -0.50062 | -0.59526 |
| 0.283 | -0.2219 | -0.2818 | -0.0799 | -0.3813 | -0.2296 | -0.3960 | -0.3363 | -0.60546 | -0.21941 |
| 0.293 | -0.0962 | -0.0024 | -0.1195 | -0.0230 | -0.3311 | -0.3903 | -0.2453 | -0.38466 | -0.38066 |
| 0.303 | -0.1065 | -0.1281 | -0.1804 | -0.2072 | -0.1372 | 0.1064 | -0.3375 | 0.024636 | -0.33179 |
| 0.313 | -0.0667 | -0.1154 | -0.1116 | -0.1423 | -0.2253 | -0.0453 | -0.1994 | -0.29456 | -0.22236 |
| 0.323 | -0.1115 | -0.1732 | -0.1883 | -0.0820 | -0.3047 | -0.0336 | -0.2360 | -0.32028 | -0.51849 |
| 0.333 | -0.1041 | -0.1855 | -0.2300 | -0.1566 | -0.3305 | -0.0807 | -0.1888 | -0.41706 | -0.24192 |
| 0.343 | -0.1654 | -0.0938 | -0.0993 | -0.1716 | -0.1247 | -0.1301 | -0.1145 | -0.30848 | -0.39944 |
| 0.353 | -0.1000 | -0.1126 | -0.1040 | -0.1674 | -0.3327 | -0.1808 | -0.3129 | -0.12079 | -0.34214 |
| 0.363 | -0.0407 | -0.1629 | -0.1350 | -0.2501 | -0.2538 | -0.1908 | -0.2440 | -0.17955 | -0.41741 |
| 0.373 | -0.0680 | -0.2526 | -0.3165 | -0.0838 | -0.2997 | -0.3696 | -0.2451 | -0.15767 | -0.39906 |
| 0.383 | -0.2081 | -0.1578 | -0.1149 | -0.3506 | -0.1866 | -0.0558 | -0.3224 | -0.64034 | -0.30142 |
| 0.393 | -0.1019 | -0.0832 | -0.0874 | -0.2070 | -0.1618 | -0.1723 | -0.1952 | -0.19927 | -0.28748 |
| 0.403 | -0.1378 | -0.2905 | -0.2551 | -0.2032 | -0.2532 | -0.0428 | -0.2711 | -0.18207 | -0.39428 |
| 0.413 | -0.0191 | 0.0304 | -0.0381 | -0.2509 | -0.1174 | -0.0466 | -0.2703 | -0.23013 | -0.36736 |
| 0.423 | -0.0980 | -0.3107 | -0.3365 | -0.0140 | -0.5869 | -0.0746 | -0.1727 | -0.3001 | -0.45199 |
| 0.433 | -0.1014 | -0.0925 | -0.1135 | -0.3960 | 0.0275 | -0.4036 | -0.2355 | -0.69046 | -0.12025 |
| 0.443 | -0.1331 | -0.0382 | -0.1719 | -0.0643 | -0.3519 | -0.3086 | -0.1456 | 0.038981 | -0.39967 |
| 0.453 | -0.1130 | -0.1053 | -0.1175 | -0.3026 | -0.0061 | -0.3366 | -0.4538 | -0.29969 | -0.2492 |
| 0.463 | -0.0725 | -0.1500 | -0.1631 | -0.0174 | -0.1074 | -0.3110 | -0.2024 | -0.33924 | -0.40319 |
| 0.473 | -0.1095 | -0.1550 | -0.3061 | -0.2046 | -0.1152 | -0.2532 | -0.4059 | -0.37237 | -0.34013 |
| 0.483 | -0.1243 | -0.1258 | -0.0113 | -0.1585 | -0.2678 | -0.3425 | 0.0063 | -0.40029 | -0.32257 |
| 0.493 | -0.1043 | -0.0600 | -0.2340 | -0.3363 | -0.1507 | -0.2359 | -0.2901 | -0.10521 | -0.35117 |

| Time | 26 | 29 | 31 | 34 | 36 | 38 | 40 | 42 | 43 |
|---|---|---|---|---|---|---|---|---|---|
| 0.003 | -0.04696 | -0.04696 | -0.04696 | -0.04696 | -0.04696 | -0.04696 | -0.04696 | -0.04696 | -0.04696 |
| 0.013 | 0.059283 | 0.086638 | 0.10715 | 0.1398 | 0.16402 | 0.18961 | 0.21589 | 0.237 | 0.25893 |
| 0.023 | 0.18524 | 0.24352 | 0.28629 | 0.35623 | 0.40595 | 0.45781 | 0.5113 | 0.55386 | 0.59945 |
| 0.033 | 0.21864 | 0.2824 | 0.32937 | 0.40559 | 0.4585 | 0.51516 | 0.57677 | 0.62439 | 0.67401 |
| 0.043 | 0.017403 | 0.028296 | 0.045017 | 0.066388 | 0.088191 | 0.11947 | 0.14194 | 0.16429 | 0.18678 |
| 0.053 | -0.25172 | -0.26962 | -0.28025 | -0.29955 | -0.31319 | -0.32429 | -0.34232 | -0.35426 | -0.36673 |
| 0.063 | -0.12299 | -0.13234 | -0.1319 | -0.15971 | -0.17191 | -0.16752 | -0.19505 | -0.20295 | -0.2129 |
| 0.073 | -0.15776 | -0.1612 | -0.18737 | -0.24938 | -0.27594 | -0.29723 | -0.31379 | -0.32097 | -0.31581 |
| 0.083 | -0.15781 | -0.14735 | -0.12067 | -0.15845 | -0.20316 | -0.24918 | -0.2973 | -0.33202 | -0.35983 |
| 0.093 | -0.1591 | -0.29638 | -0.2108 | -0.075096 | -0.047811 | -0.0055604 | -0.0051937 | -0.0041273 | -0.013281 |
| 0.103 | -0.27069 | -0.26142 | -0.22863 | -0.085277 | -0.10774 | -0.12738 | -0.11444 | -0.12271 | -0.16031 |
| 0.113 | -0.1448 | -0.21503 | -0.17416 | -0.1067 | -0.27511 | -0.36827 | -0.24439 | -0.19732 | -0.10783 |
| 0.123 | -0.20821 | -0.13008 | -0.29887 | -0.56902 | -0.49549 | -0.53159 | -0.54084 | -0.74037 | -0.57435 |
| 0.133 | -0.13569 | -0.3339 | -0.2078 | -0.32652 | -0.36955 | -0.41794 | -0.34986 | -0.46729 | -0.45948 |
| 0.143 | -0.17772 | -0.13066 | -0.2789 | -0.43972 | -0.49293 | -0.44337 | -0.46547 | -0.52855 | -0.7046 |
| 0.153 | -0.20638 | -0.25566 | -0.24601 | -0.26462 | -0.43451 | -0.59312 | -0.55449 | -0.71229 | -0.24591 |
| 0.163 | -0.19209 | -0.31886 | -0.26775 | -0.17753 | -0.45967 | -0.34685 | -0.4541 | -0.37571 | -0.51242 |
| 0.173 | -0.27379 | -0.23822 | -0.33405 | -0.42646 | -0.23127 | -0.55349 | -0.45313 | -0.34897 | -0.34801 |
| 0.183 | -0.23043 | -0.1867 | -0.22222 | -0.28593 | -0.40002 | -0.25334 | -0.35706 | -0.24085 | -0.59694 |
| 0.193 | -0.16897 | -0.12049 | -0.27655 | -0.35003 | -0.27825 | -0.39306 | -0.29624 | -0.41953 | -0.49014 |
| 0.203 | -0.18115 | -0.35167 | -0.24386 | -0.31651 | -0.28578 | -0.2201 | -0.35887 | -0.52059 | -0.33357 |
| 0.213 | -0.17336 | -0.26802 | -0.22412 | -0.39078 | -0.3637 | -0.36231 | -0.45262 | -0.37074 | -0.544 |
| 0.223 | -0.16021 | -0.24369 | -0.23456 | -0.44495 | -0.37374 | -0.54645 | -0.32441 | -0.43641 | -0.24548 |
| 0.233 | -0.16157 | -0.25117 | -0.23971 | -0.32728 | -0.43578 | -0.45338 | -0.32202 | -0.20627 | -0.77985 |
| 0.243 | -0.17774 | -0.19418 | -0.25529 | -0.31894 | -0.18305 | -0.40332 | -0.42656 | -0.40835 | -0.28757 |
| 0.253 | -0.29924 | -0.32295 | -0.3053 | -0.28165 | -0.47809 | -0.2803 | -0.25493 | -0.52206 | -0.50875 |
| 0.263 | -0.27668 | -0.15165 | -0.2646 | -0.23524 | -0.2748 | -0.45534 | -0.38184 | -0.27044 | -0.50687 |
| 0.273 | -0.26055 | -0.27629 | -0.21536 | -0.38077 | -0.35578 | -0.54881 | -0.38455 | -0.10891 | -0.6651 |
| 0.283 | -0.069408 | -0.24141 | -0.22805 | -0.46111 | -0.42213 | -0.39195 | -0.5195 | -0.43306 | -0.64342 |
| 0.293 | -0.19547 | -0.16239 | -0.23576 | -0.2765 | -0.15078 | -0.3791 | -0.52315 | -0.57102 | -0.22859 |
| 0.303 | -0.21344 | -0.36946 | -0.39733 | -0.28738 | -0.55297 | -0.33344 | -0.19994 | -0.42731 | -0.44635 |
| 0.313 | -0.21766 | -0.1246 | -0.3793 | -0.32146 | -0.11175 | -0.38001 | -0.38292 | -0.20537 | -0.38976 |
| 0.323 | -0.17127 | -0.31643 | -0.28342 | -0.24344 | -0.52884 | -0.39632 | -0.1689 | -0.32062 | -0.4387 |
| 0.333 | -0.21634 | -0.18469 | -0.28203 | -0.30824 | -0.21006 | -0.43084 | -0.45441 | -0.47707 | -0.63956 |
| 0.343 | -0.18518 | -0.27881 | -0.19626 | -0.32066 | -0.41562 | -0.58653 | -0.36849 | -0.43383 | -0.4279 |
| 0.353 | -0.22345 | -0.38579 | -0.28603 | -0.45264 | -0.46901 | -0.35841 | -0.32112 | -0.39827 | -0.55536 |
| 0.363 | -0.14059 | -0.21741 | -0.2916 | -0.3923 | -0.32984 | -0.32568 | -0.57567 | -0.57972 | -0.33144 |
| 0.373 | -0.22394 | -0.17828 | -0.35339 | -0.31879 | -0.34166 | -0.44248 | -0.45458 | -0.48836 | -0.3989 |
| 0.383 | -0.2075 | -0.11152 | -0.20491 | -0.19829 | -0.31218 | -0.38348 | -0.32536 | -0.41182 | -0.75882 |
| 0.393 | -0.14619 | -0.3599 | -0.27356 | -0.36782 | -0.53199 | -0.33109 | -0.17913 | -0.60344 | -0.58204 |
| 0.403 | -0.16643 | -0.071452 | -0.23184 | -0.38401 | -0.28624 | -0.40331 | -0.61297 | -0.40288 | -0.52819 |
| 0.413 | -0.13792 | -0.26384 | -0.2947 | -0.3401 | -0.48368 | -0.46684 | -0.3781 | -0.63091 | -0.44338 |
| 0.423 | -0.28696 | -0.15474 | -0.37235 | -0.26493 | -0.18972 | -0.52417 | -0.4684 | -0.38473 | -0.50504 |
| 0.433 | -0.21089 | -0.33387 | -0.26768 | -0.22449 | -0.42759 | -0.42596 | -0.44599 | -0.7083 | -0.60793 |
| 0.443 | -0.1581 | -0.20351 | -0.38915 | -0.2764 | -0.39804 | -0.3884 | -0.096908 | -0.20146 | -0.44806 |
| 0.453 | -0.2063 | -0.24461 | -0.2067 | -0.28265 | -0.26002 | -0.45793 | -0.41048 | -0.54703 | -0.49019 |
| 0.463 | -0.20989 | -0.16262 | -0.2672 | -0.40287 | -0.48794 | -0.43786 | -0.34904 | -0.4963 | -0.38611 |
| 0.473 | -0.19175 | -0.22972 | -0.28082 | -0.21441 | -0.29048 | -0.29887 | -0.54296 | -0.4546 | -0.60945 |
| 0.483 | -0.20397 | -0.28252 | -0.21166 | -0.22384 | -0.44371 | -0.3568 | -0.32728 | -0.54812 | -0.56805 |
| 0.493 | -0.17066 | -0.1334 | -0.20657 | -0.14761 | -0.39552 | -0.35501 | -0.25154 | -0.14077 | -0.60829 |

| Time | 26 | 29 | 31 | 34 | 36 | 38 | 40 | 41.5 | 43 |
|---|---|---|---|---|---|---|---|---|---|
| 0.003 | -0.03669 | -0.03669 | -0.03669 | -0.03669 | -0.03669 | -0.03669 | -0.03669 | -0.03669 | -0.03669 |
| 0.013 | 0.12184 | 0.16338 | 0.19387 | 0.242 | 0.27766 | 0.31549 | 0.35583 | 0.38564 | 0.39626 |
| 0.023 | 0.35496 | 0.44864 | 0.51938 | 0.63361 | 0.71765 | 0.80658 | 0.89902 | 0.96756 | 0.98923 |
| 0.033 | 0.50232 | 0.62679 | 0.71695 | 0.87052 | 0.97776 | 1.0909 | 1.2079 | 1.301 | 1.3301 |
| 0.043 | 0.29009 | 0.38191 | 0.44978 | 0.55728 | 0.63547 | 0.71684 | 0.80605 | 0.87634 | 0.90289 |
| 0.053 | 0.029197 | 0.10731 | 0.17613 | 0.2679 | 0.34365 | 0.41506 | 0.49896 | 0.5619 | 0.58426 |
| 0.063 | -0.19853 | -0.19413 | -0.17876 | -0.1488 | -0.11683 | -0.092057 | -0.044916 | -0.0043221 | 0.013496 |
| 0.073 | -0.29387 | -0.35456 | -0.3796 | -0.39261 | -0.40179 | -0.40834 | -0.39245 | -0.3745 | -0.37181 |
| 0.083 | -0.33886 | -0.45436 | -0.52042 | -0.55996 | -0.44051 | -0.30595 | -0.22506 | -0.23912 | -0.20399 |
| 0.093 | 0.035873 | -0.066079 | -0.15558 | -0.25738 | -0.30054 | -0.30336 | -0.23173 | -0.1473 | -0.1516 |
| 0.103 | -0.1956 | -0.21352 | -0.28717 | -0.41388 | -0.42321 | -0.50699 | -0.71623 | -0.6054 | -0.62713 |
| 0.113 | -0.14895 | -0.21997 | -0.18791 | -0.31436 | -0.39814 | -0.58865 | -0.73741 | -0.66751 | -0.66265 |
| 0.123 | -0.3732 | -0.13151 | -0.21499 | -0.2072 | -0.41911 | -0.49588 | -0.21854 | -0.30041 | -0.30633 |
| 0.133 | -0.27283 | -0.41762 | -0.46299 | -0.58632 | -0.4888 | -0.52467 | -0.62929 | -0.62203 | -0.64055 |
| 0.143 | -0.14641 | -0.34305 | -0.40011 | -0.41692 | -0.5904 | -0.57885 | -0.58638 | -0.56429 | -0.60495 |
| 0.153 | -0.2469 | -0.11591 | -0.18263 | -0.37318 | -0.28693 | -0.44517 | -0.41277 | -0.31919 | -0.33533 |
| 0.163 | -0.18022 | -0.30915 | -0.2635 | -0.37204 | -0.39473 | -0.46392 | -0.73393 | -0.71225 | -0.71744 |
| 0.173 | -0.24895 | -0.20304 | -0.40511 | -0.31884 | -0.39067 | -0.52401 | -0.3392 | -0.56471 | -0.59804 |
| 0.183 | -0.19459 | -0.20112 | -0.24133 | -0.39876 | -0.35639 | -0.47378 | -0.50993 | -0.37921 | -0.38697 |
| 0.193 | -0.2084 | -0.30392 | -0.26074 | -0.22073 | -0.44406 | -0.5006 | -0.4341 | -0.52879 | -0.55839 |
| 0.203 | -0.22435 | -0.18185 | -0.32689 | -0.41391 | -0.25779 | -0.43476 | -0.49061 | -0.54222 | -0.51746 |
| 0.213 | -0.19847 | -0.33711 | -0.31207 | -0.31687 | -0.4576 | -0.38008 | -0.57991 | -0.5674 | -0.56244 |
| 0.223 | -0.23975 | -0.19232 | -0.35839 | -0.31339 | -0.30402 | -0.50275 | -0.45686 | -0.62506 | -0.69073 |
| 0.233 | -0.20411 | -0.27261 | -0.27847 | -0.41504 | -0.38719 | -0.42948 | -0.51198 | -0.46386 | -0.42506 |
| 0.243 | -0.20908 | -0.29262 | -0.3138 | -0.29133 | -0.48101 | -0.41842 | -0.46703 | -0.57385 | -0.59332 |
| 0.253 | -0.24138 | -0.21725 | -0.33445 | -0.39071 | -0.25173 | -0.48287 | -0.46745 | -0.52088 | -0.54912 |
| 0.263 | -0.18361 | -0.34173 | -0.29372 | -0.35257 | -0.52538 | -0.41107 | -0.50809 | -0.50213 | -0.48545 |
| 0.273 | -0.24342 | -0.19937 | -0.29874 | -0.32909 | -0.29505 | -0.43141 | -0.45154 | -0.53826 | -0.60387 |
| 0.283 | -0.20804 | -0.32479 | -0.29319 | -0.37933 | -0.38186 | -0.50407 | -0.55618 | -0.54473 | -0.53198 |
| 0.293 | -0.20466 | -0.22992 | -0.32258 | -0.35689 | -0.47266 | -0.38056 | -0.40099 | -0.45701 | -0.47648 |
| 0.303 | -0.24065 | -0.22012 | -0.26868 | -0.34622 | -0.25883 | -0.46573 | -0.54553 | -0.57181 | -0.61472 |
| 0.313 | -0.19769 | -0.33782 | -0.32474 | -0.37582 | -0.49683 | -0.48455 | -0.48385 | -0.56436 | -0.55144 |
| 0.323 | -0.22626 | -0.15922 | -0.30559 | -0.37257 | -0.32379 | -0.36621 | -0.42841 | -0.43267 | -0.46189 |
| 0.333 | -0.22672 | -0.34332 | -0.284 | -0.32141 | -0.42268 | -0.53168 | -0.59767 | -0.64448 | -0.64729 |
| 0.343 | -0.20899 | -0.21992 | -0.34241 | -0.40229 | -0.3586 | -0.43125 | -0.36025 | -0.44182 | -0.44053 |
| 0.353 | -0.2258 | -0.25944 | -0.25855 | -0.33773 | -0.3776 | -0.39121 | -0.56527 | -0.53128 | -0.56673 |
| 0.363 | -0.22415 | -0.31718 | -0.33492 | -0.3492 | -0.40341 | -0.5565 | -0.50583 | -0.61953 | -0.61206 |
| 0.373 | -0.21131 | -0.19162 | -0.30216 | -0.40656 | -0.33275 | -0.35387 | -0.36827 | -0.38115 | -0.40435 |
| 0.383 | -0.23028 | -0.32293 | -0.25996 | -0.29756 | -0.4609 | -0.4709 | -0.64186 | -0.65526 | -0.67051 |
| 0.393 | -0.22378 | -0.20605 | -0.36019 | -0.40843 | -0.35773 | -0.51309 | -0.39122 | -0.49431 | -0.49656 |
| 0.403 | -0.20716 | -0.29431 | -0.26437 | -0.3615 | -0.43277 | -0.34095 | -0.47346 | -0.43445 | -0.46034 |
| 0.413 | -0.24041 | -0.23665 | -0.29857 | -0.30834 | -0.39303 | -0.53236 | -0.59099 | -0.68399 | -0.69435 |
| 0.423 | -0.21112 | -0.24895 | -0.3417 | -0.44052 | -0.35179 | -0.43821 | -0.38036 | -0.40983 | -0.41008 |
| 0.433 | -0.21716 | -0.30823 | -0.2622 | -0.31054 | -0.45733 | -0.3748 | -0.52991 | -0.52254 | -0.55444 |
| 0.443 | -0.23872 | -0.22439 | -0.32736 | -0.35812 | -0.30776 | -0.55545 | -0.5314 | -0.62733 | -0.63544 |
| 0.453 | -0.19887 | -0.31206 | -0.31439 | -0.42239 | -0.4499 | -0.38188 | -0.40624 | -0.41189 | -0.41026 |
| 0.463 | -0.23586 | -0.23464 | -0.27367 | -0.29557 | -0.40529 | -0.42869 | -0.55129 | -0.58037 | -0.62055 |
| 0.473 | -0.22208 | -0.28113 | -0.33795 | -0.4041 | -0.31489 | -0.53478 | -0.4936 | -0.56398 | -0.55772 |
| 0.483 | -0.2018 | -0.26821 | -0.29976 | -0.37959 | -0.49346 | -0.35945 | -0.42173 | -0.42604 | -0.43685 |
| 0.493 | -0.24509 | -0.21886 | -0.28151 | -0.30695 | -0.32408 | -0.49041 | -0.58593 | -0.63381 | -0.66745 |

# References


Alam, F et al. (2010). "Aerodynamics of used cricket balls". In: *Proc. 17th Australasian Fluid Mechanics Conf.(Auckland, New Zealand, 5–9 December 2010)*.

Barrett, R.S and D.H Wood (1996). "The theory and practice of reverse swing". In: *Sports Coach* 18, pp. 28–30.

Barton, N. G. (1982). "On the Swing of a Cricket Ball in Flight". In: *Proceedings of the Royal Society of London A: Mathematical, Physical and Engineering Sciences* 379.1776, pp. 109–131. ISSN: 0080-4630. DOI: 10.1098/rspa.1982.0008. eprint: http://rspa.royalsocietypublishing.org/content/379/1776/109.full.pdf. URL: http://rspa.royalsocietypublishing.org/content/379/1776/109.

Binnie, A.M. (1976). "The effect of humidity on the 'swing' of cricket balls". In: *International Journal of Mechanical Sciences* 18.9, pp. 497–499. ISSN: 0020-7403. DOI: http://dx.doi.org/10.1016/0020-7403(76)90046-1. URL: http://www.sciencedirect.com/science/article/pii/0020740376900461.

Center, Glen Research (2017a). *Drag of a Sphere*. URL: https://www.grc.nasa.gov/www/K-12/airplane/dragsphere.html (visited on 03/17/2017).

— (2017b). *Mach Role*. URL: https://www.grc.nasa.gov/www/k-12/airplane/machrole.html (visited on 01/26/2017).

Cooke, J.C. (1955). "The Boundary Layer and "Seam" Bowling". In: *The Mathematical Gazette* 39.329, pp. 196–199. DOI: 10.2307/3608746.

Cork, Alexander, Laura Justham, and Andrew West (2013). "Three-dimensional vision analysis to measure the release characteristics of elite bowlers in cricket". In: *Proceedings of the Institution of Mechanical Engineers, Part P: Journal of Sports Engineering and Technology* 227.2, pp. 116–127. DOI: 10.1177/1754337112447264. URL: http://dx.doi.org/10.1177/1754337112447264.

Franzini, J.B., E.J. Finnemore, and R.L. Daugherty (1997). *Fluid mechanics with engineering applications*. McGraw-Hill. ISBN: 9780070219144.

James, David, Danielle C. MacDonald, and John Hart (2012). "The effect of atmospheric conditions on the swing of a cricket ball". In: *Procedia Engineering* 34, pp. 188–193. ISSN: 1877-7058. DOI: http://dx.doi.org/10.1016/j.proeng.2012.04.033. URL: http://www.sciencedirect.com/science/article/pii/S1877705812016463.

K. Bentley P. Varty, M. Proudlove and R. D. Mehta. (1982). "An experimental study of cricket ball swing". In: *Imperial College Aero Technical Note*, pp. 82–106.

K Sherwin, J L Sproston (1982). "Aerodynamics of a cricket ball". In: *International Journal of Mechanical Enineering Education* 10, pp. 71–79.

Latchman, Richie and Akash Pooransingh. "Modeling Conventional Swing of a Cricket Ball Using COMSOL Multiphysics". In: *COMSOL Blog*.

Mehta, R D (1985). "Aerodynamics of Sports Balls". In: *Annual Review of Fluid Mechanics* 17.1, pp. 151–189. DOI: 10.1146/annurev.fl.17.010185.001055. eprint: http://dx.doi.org/10.1146/annurev.fl.17.010185.001055. URL: http://dx.doi.org/10.1146/annurev.fl.17.010185.001055.

Mehta, R.D (2006a). "Swinging it three ways". In: *The Wisden Cricketer* 3.10, pp. 50–53.

— (2006b). "The science of swing bowling". In: *ESPNCricinfo*.

— (2014). "Fluid Mechanics of Cricket Ball Swing". In: *19th Australasian Fluid Mechanics Conference*.

Mehta, R.D and D Wood (1980). "Aerodynamics of the Cricket Ball". In: *New Scientist* 87.1213, pp. 442–447.

Menter, Florian R (1994). "Two-equation eddy-viscosity turbulence models for engineering applications". In: *AIAA journal* 32.8, pp. 1598–1605.

Menter, Florian R (2009). "Review of the shear-stress transport turbulence model experience from an industrial perspective". In: *International Journal of Computational Fluid Dynamics* 23.4, pp. 305–316.

Menter, FR, M Kuntz, and R Langtry (2003). "Ten years of industrial experience with the SST turbulence model". In: *Turbulence, heat and mass transfer* 4.1, pp. 625–632.

Online, CFD (2005a). *SimpleFoam General Properties*. URL: http://www.cfdsupport.com/OpenFOAM-Training-by-CFD-Support/node158.html (visited on 12/02/2016).

— (2005b). *SST k-omega Model*. URL: http://www.cfd-online.com/Wiki/SST_k-omega_model (visited on 11/25/2016).

Pahinkar, D G and J Srinivasan (2010). "Simulation of Reverse Swing of the Cricket Ball". In: *International Journal of Sports Science and Engineering* 4.1, pp. 53–64.

Patankar, S.V and D.B Spalding (1972). "A calculation procedure for heat, mass and momentum transfer in three-dimensional parabolic flows". In: *International Journal of Heat and Mass Transfer* 15.10, pp. 1787–1806. ISSN: 0017-9310. DOI: http://dx.doi.org/10.1016/0017-9310(72)90054-3. URL: http://www.sciencedirect.com/science/article/pii/0017931072900543.

Penrose, J.M.T., D.R. Hose, and E.A. Trowbridge (1996). "Cricket ball swing: A preliminary analysis using computational fluid dynamics". In: *Engineering of Sport, International Conference, 1*, pp. 11–19.

Robinson, Garry and Ian Robinson (2015). "The effect of spin in swing bowling in cricket: model trajectories for spin alone". In: *Physica Scripta* 90.2, p. 028004. URL: http://stacks.iop.org/1402-4896/90/i=2/a=028004.

Sayers, A T (2001). "On the reverse swing of a cricket ball—modelling and measurements". In: *Proceedings of the Institution of Mechanical Engineers, Part C: Journal of Mechanical Engineering Science* 215.1, pp. 45–55. DOI: 10.1243/0954406011520508. eprint: http://dx.doi.org/10.1243/0954406011520508. URL: http://dx.doi.org/10.1243/0954406011520508.

Sayers, A.T and A Hill (1999). "Aerodynamics of a cricket ball". In: *Journal of Wind Engineering and Industrial Aerodynamics* 79.1–2, pp. 169–182. ISSN: 0167-6105. DOI: http://dx.doi.org/10.1016/S0167-6105(97)00299-7. URL: //www.sciencedirect.com/science/article/pii/S0167610597002997.

Scobie, James A et al. (2013). "Fluid dynamics of cricket ball swing". In: *Proceedings of the Institution of Mechanical Engineers, Part P: Journal of Sports Engineering and Technology* 227.3, pp. 196–208. DOI: 10.1177/1754337112462320. eprint: http://dx.doi.org/10.1177/1754337112462320. URL: http://dx.doi.org/10.1177/1754337112462320.

*Specification for cricket balls* (1995). BS 5993:1994. British Standards Institute.

*The Laws of the cricket: Law 5 the Ball*. Marylebone Cricket Club.